

THESIS FOR THE DEGREE OF DOCTOR OF PHILOSOPHY

# Co-Processing Fat-rich Material into Diesel Fuel

SHANMUGAM PALANISAMY



**CHALMERS**

Applied Surface Chemistry  
Department of Chemical and Biological Engineering  
Chalmers University OF Technology  
Göteborg, Sweden 2013

CO-PROCESSING FAT-RICH MATERIAL INTO DIESEL FUEL  
SHANMUGAM PALANISAMY

ISBN 978-91-7385-837-3

©SHANMUGAM PALANISAMY, 2013.

Doktorsavhandlingar vid Chalmers tekniska högskola

Ny serie nr 3518

ISSN 0346-718X

Applied Surface Chemistry  
Department of Chemical and Biological Engineering  
Chalmers University of Technology,  
SE-412 96,  
Göteborg,  
Sweden,  
Telephone: +46(0)31-7721000

Cover:

Conventional and Renewable resources into diesel fuel

Göteborg,  
Sweden 2013

*To the memory of my Grandfather*

## Abstract

The thesis concerns aspects of method for increased use of alternative fat-rich material in diesel fuel and improve the cold properties of down-stream co-processed diesel fuel. The PhD thesis is a part of 'Towards sustainable bio-refinery' group which is funded by Preem AB and Swedish Energy Agency. Co-processing of fat-rich material into renewable fuel to scale-up refinery infrastructure with number of benefits like enrich the renewable carbon content, remove environmentally concerned heteroatom, improve the quality of fuel and reduce the dependency of conventional fossil fuels. The research focused to minimize the H<sub>2</sub> dependent for upgrading process. In relation to minimize H<sub>2</sub> consumption, it is experimented with Fatty Acid Methyl Ester (FAME) and/or rapeseed oil to hydroprocess carboxyl group in thermal treatment, followed with catalytic hydroprocessing.

From our result, it shows that FAME and/or rapeseed oil on medium temperature (300 to 370°C) without any catalyst gives lighter cracking and cyclic group formation with longer contact time on inert material. From the result,  $\alpha$ - and  $\beta$ -carbon breakage is evidence during thermal decomposition without any effect by H<sub>2</sub> partial pressure. Here, Decarbonylation involved during thermal cracking without effect of H<sub>2</sub> partial pressure and catalyst. Increase in CO in a gas outlet confirms the breakage in the  $\alpha$ -carbonyl group during high temperature. To conclude, Pre-heating technique on fat-rich material influences a significant part of the upgrading process with or without limited H<sub>2</sub> use.

Catalytic hydroprocessing of FAME and/or rapeseed oil at operating temperature of 350°C between 4.0 and 10.0 Mpa total pressures with a sulfide NiMo/ $\gamma$ -Al<sub>2</sub>O<sub>3</sub> catalyst results to retain a selective product in the form of C<sub>15</sub>, C<sub>16</sub>, C<sub>17</sub> and C<sub>18</sub> with traces of lighter hydrocarbons. This catalyst has stronger activity on carboxyl group compare on C-C group.

Tall oil FAME is already an established diesel fuel additive but apart from the highly functional FAME, the processing of tall oil also gives a heavier fraction of resin acids. In a project studied the hydroprocessing of a mixture of 10-30 % of FAME and/or tall oil with Light gas oil (LGO) in a catalytic reactor using NiMo/ $\gamma$ -Al<sub>2</sub>O<sub>3</sub> like catalyst. This experiment was run for different temperatures (300 °C to 405 °C) and different flow rates. Different aspects have been studied from the results: weight percentage of hydrocarbons C<sub>17</sub> and C<sub>18</sub> in the product, sulphur and aromatics contents, the cloud point and volume percentage for gas products like methane, CO<sub>2</sub> and CO. The resin acids, modeled by abietic acid, can be catalytically hydrogenated. The resin acid fraction relatively end-up with mono- and di-aromatics but restricted to Poly-aromatics formation.

Isomerization of higher alkanes leads into branched compounds to narrow diesel fraction and reduce cloud point. Bi-functional catalyst prepared with zeolite show immersive isomeric catalytic properties in last decades. The special feature of the zeolite, which has weak acidic sites, enhance Bronsted acidity leads low coking on active sites. The selectivity of product has been studied with structure and pore dimension depends on high Silica content. The test over 10 wt% n-hexadecane in LGO was studied by adjusting temperature, space velocity and pressure parameter. The result concludes that moderate temperature (230°C to 270°C) and pressure between 4.0 and 7.0 MPa have yielded better reaction condition. The isomeric group selectivity peak at 250°C considered as optimum for high yield of isomeric group in relation to cracking as undesired mechanism. Isomeric naphtha like ethylene, i-pentane, i-butane were observed in fuel gas outlet.

**Keywords:** Hydroprocessing, Fatty Acid Methyl Ester, Tall oil, Rapeseed oil, Decarbonylation, Decarboxylation, Deoxygenation, Isomerization.

### List of Publications

1. Temperature dependent by decarboxylation and decarbonylation of rapeseed oil on inert material in H<sub>2</sub> partial pressure- *Submitted in Journal of Fuel*.
2. Shanmugam Palanisamy and Börje S. Gevert, Hydro treatment of Rapeseed Oil, World Renewable Energy Congress-2011, May 09-13, Linkoping, Sweden.
3. Hydrogenation and Decarboxylation/Decarbonylation of Rapeseed Oil – presence or absence of NiMoS/ $\gamma$ -Al<sub>2</sub>O<sub>3</sub>- *Submitted in Journal of Fuel*.
4. Hydroprocessing of Fatty acid methyl ester in gas oil blend – NiMoS/Alumina catalyst-*Submitted in Journal of Fuel Processing Technology*.
5. Hydroprocessing of Fatty acid methyl ester containing resin acids in gas oil blend – NiMoS/Alumina catalyst-*Submitted in Journal of Fuel Processing Technology*.
6. Isomerization of n-C<sub>16</sub> in light gas oil with beta zeolite – *Manuscript*.

### Contribution Report

1. All experimental work with analytical study and writing manuscript.
2. All experimental work with analytical study and writing manuscript.
3. All experimental work with analytical study and writing a part of manuscript.
4. All experimental work with analytical study and writing a part of manuscript.
5. All experimental work with analytical study and writing a part of manuscript.
6. All experimental work with analytical study and writing a part of manuscript.

**Publication not Included in this Thesis**

1. Thermal and Catalytic deoxygenation Of Rapeseed Oil, 7th Asia pacific Conference on Sustainable Energy and Environmental Technologies, Oct. 15-19, 2009, Qingdao, China.
2. Fischer-Tropsch synthesis with simultaneous water gas shift reaction, Prepr. Pap.-Am. Chem. Soc., Div. Pet. Chem. 2010, 55(1).
3. Hydro-cracking of Rapeseed oil, The Renewable Energy Research Conference 2010, June 7th - 8th 2010, Trondheim, Norway.
4. Alkylation of ethylene with zeolite Beta, International Conference on Biology, Environment and Chemistry (ICBEC 2010), Hong Kong, China, December 28 - 30, 2010.

## Chapter

1. Introduction.....	1-1
2. Feed Materials.....	2-5
2.1. Fatty Acid Methyl Ester .....	2-5
2.2. Rosin Acids.....	2-5
2.3. Rapeseed Oil.....	2-7
2.4. Light Light Gas Oil (LLGO) .....	2-7
2.5. Hexadecane.....	2-8
2.6. HDN-60 Catalyst .....	2-8
2.7. Zeolite Catalyst.....	2-9
3. Experimental Methods .....	3-10
3.1. Batch Reactor .....	3-10
3.2. Fixed-bed Reactor.....	3-11
3.3. Liquid Analytical Methods .....	3-11
3.4. Gas Analytical Method.....	3-12
3.5. Distillation Methods .....	3-13
3.6. Soxhlet Method.....	3-13
3.7. Characterization Techniques .....	3-13
3.8. Hydroprocessing Catalyst- NiMo/Alumina.....	3-14
3.9. Hydroisomerization Catalyst- H-beta Zeolite.....	3-15
3.10. Overview of the Experiments .....	3-17
4. Thermal Decomposition.....	4-19
4.1. Thermal Treatment .....	4-19
4.2. Thermal Decomposition .....	4-24
5. Catalytic Hydrotreating Process .....	5-26
5.1. Fatty Acid Methyl Ester Hydroprocessing .....	5-26
5.2. Rosin Acids Hydroprocessing .....	5-27
5.3. CO and CO <sub>2</sub> in Fuel Gas.....	5-28
5.4. Decarboxylation and Decarbonylation .....	5-29
5.5. Deoxygenation and Desulphurization .....	5-30
6. n-Paraffin Upgrading Process .....	6-33
6.1. Thermal-Cracking.....	6-33
6.2. Hydroisomerization .....	6-34
6.3. Isomeric Lighter Fraction in Fuel Gas.....	6-35
7. Conclusion .....	7-36
8. Acknowledgments.....	8-46



# CHAPTER 1

## Introduction

### 1. Introduction

The discovery of crude oil in the 19<sup>th</sup> century established an inexpensive liquid fuel source that helped industrialize the world and improve standards of living. Before the discovery of inexpensive fossil fuels, our society was dependent on renewable sources to meet its energy needs. Because of the increasing demand of petroleum fuels by developing economics and political and environmental concerns about fossil fuels, it is imperative to develop economic and energy efficient processes for the sustainable production of fuels and chemicals [1-8].

At present, crude oil exploration has been increased to 30 billion barrels per year and the discovery rate is now approaching 4 billion barrels of crude oil per year. The petroleum industries commenced with exploration, extraction, refining and marketing of various products, which accounts for major energy consumption in various sectors (e.g., industry, transportation, agriculture and household use) [5-7]. In general, explored Crude oil is the main source as conventional fuels such as fuel gas, gasoline, diesel and heavy oil. Nearly one third of the demand for crude oil is from the transportation sector (e.g., cars, trucks, buses and the marine industry). The demand for transportation fuels increases exponentially by economic growth, attention is to create substantial requirement of excess fuel source for future generation demand [9-11]. Furthermore, conventional fuels lead to an increase in greenhouse emission. The presence of heteroatoms in fuel increases the hazard emission in exhaust gas. The biofuels produced from the renewable sources could help to minimize fossil fuel utilization and greenhouse gas (CO<sub>2</sub>) emissions.

Biofuels have been distinguished as first and second generation. First-generation (or conventional) biofuels (i.e. biodiesel (bio-esters) and bio-ethanol and biogas) are characterized either by their ability to be blended with petroleum-based fuels, combusted in existing internal combustion engines and distributed through existing infrastructure, or by their use in existing alternative vehicle technology (e.g., flexible fuel vehicle) or natural gas vehicles. According to 2010 statistics, biofuel has a 2.7% share in the transportation sector worldwide [12-14]. There are also other biofuels, including biogas, which is derived by

anaerobic treatment of manure and other biomass materials. However, the volumes of biogas used for transportation are relatively small. First generation biofuels can offer some CO<sub>2</sub> benefits and help to improve domestic energy security. However, there are concerns about the sourcing of feedstock, including the impact it may have on biodiversity and land use as well as competition with food crops.

The first generation bio-refinery concepts were published in a number of publications as investigations and reviews were directed toward food- and non-food-based bio-refineries. Information on the second-generation bio-refinery concepts and related chemical production has been highly emphasized in the present research scenario. The main sources for producing renewable diesel by second-generation biofuel concepts have focused on biomass, vegetable oils, waste cooking oils, black liquor waste (Tall oil), lignin extraction and other fat rich sources [15-21]. An advantage of bio-refinery concept is mainly focused to synchronise existing refinery with bio-sources within the geographical position of resource availability and the deliver product in marketing. Customizing on quality and utilization is needed to upgrade for relevant customer usage.

Biofuel is a promising renewable fuel that can be used to replace fossil diesel. Fatty acid methyl esters (FAMEs) produced through trans-esterification of vegetable oil is a first-generation biodiesel. The hydrotreatment process is somewhere between the first- and second-generation biofuels using vegetable oil but producing a fuel without oxygen, which is similar to fossil diesel. Synthetic diesel is a second-generation biodiesel produced by gasification of biomass followed by Fischer-Tropsch synthesis. Today, the hydrotreatment process is used after the trans-esterification process, with the goal of using diesel-like hydrocarbons.

High cetane value and energy content are the main components for the conventional diesel engine in order to produce high efficiency and to be mobile-power driven. Recent developments in the use of renewable sources to substitute and enrich conventional fuels in various sectors have increased, including in the petroleum industries [22-30]. One such development is blending FAME with diesel that has been hydrotreated to remove heteroatoms for commercial use. In addition, blending of vegetable oils (such as rapeseed oil in Europe) with diesel has widely been investigated in engine test [17, 31-33]. Different kinds of Swedish diesel fuel specifications are listed in Table 2.

**Table 2:** Swedish diesel specifications by three environmental classes according to 2006 data [17].

<b>Fuel Property</b>	<b>EC1 (winter)</b>	<b>EC1 (Summer)</b>	<b>EC2 (EN590 diesel)</b>
Cetane number	51	51	51
Cetane index	50	50	47
Density @ 15°C (kg/m <sup>3</sup> )	800 - 820	800 - 820	800 - 820
Sulphur, max (ppm. Wt)	10	10	50
Aromatics, max (%v/v)	5	5	20
PAH, max (% v/v)	0,02	0,02	0,1
Cloud point (°C)	-16	0	-
CFPP (°C)	-26	-10	-
Viscosity @ 40°C (mm <sup>2</sup> /s)	1.2 – 4.0	1.2 – 4.0	-
IBP, min (°C)	180	180	
T95, max (°C)	285	285	295

In general, two options are currently available in the hydrotreating process to utilize renewable fuels. First, a new process can simply be built to produce the hydrogenated vegetable oil diesel for subsequent blending with the final product of conventional diesel in an oil refinery [18-19]. This is known as the stand-alone option. Second, a co-processing approach can be taken in which synchronies existing downstream process like hydrotreater for upgrading renewable feedstock with diesel to remove sulphur by converting the sulphur to H<sub>2</sub>S. In this second option, capital costs may be reduced but mineral diesel capacity through the existing hydrotreatment will be reduced due to upstream losses [20-24]. Globally, five major proprietary technologies are under development, all of which are based around integration with existing refinery processing:

1. Neste Oil, Finland.
2. UOP, USA.
3. Petrobras, Brazil.
4. ConocoPhillips, Ireland.
5. IFP, France.

## **Objective and Goal of the Thesis**

The main aim of this thesis is to focus on two areas of processes that presently exist in refineries. First, the thesis focuses on thermal (Paper I, II and III) and the catalytic hydrotreating process (Paper IV and V) in which different feed materials have been investigated for impeded catalytic activity under different conditions. Second, the biofuel upgrading process has been investigated to improve the naphthenic properties (Paper VI) of biofuel for existing conditions in the refinery and for fuel application.

## **Thermal Process**

Here, thermal treatment of tall or vegetable oil is investigated in order to understand thermal cracking during heat-up in pre-heaters or reactor inlets. The morphological change in the carboxylic group of renewable fuels is of particular interest.

## **Catalytic Process**

In this section, commercially available catalysts (e.g., HDN-60) are used for testing in hydroprocessing. The hydrotreating process includes deoxygenation, hydrogenation and decarboxylation (DCO) and these are investigated under different conditions, especially temperature, pressure and space velocity. Further, kinetic studies are of importance in order to understanding the rate of reaction.

## **Upgrading**

Relevant to the catalytic process, the products are upgraded with zeolite catalysts and studied under different processing conditions, which play a crucial role in the variation of Paraffinic properties of the downstream diesel. Light gas oil is the main solvent and standard blended diesel is used in all of the investigations.

# CHAPTER 2

## Material used in the study

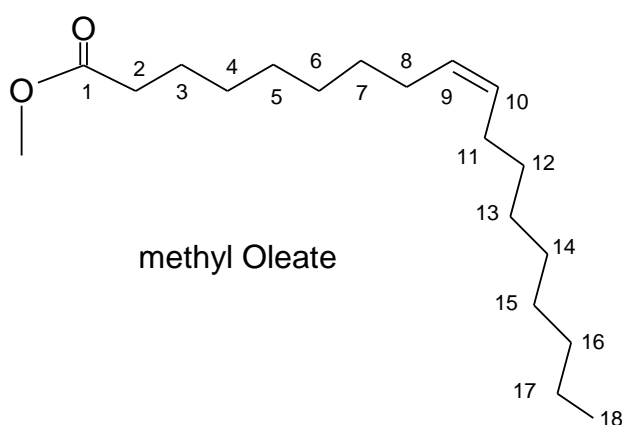
### 2. Feed Materials

The main sources for feedstock were vegetable oil, FAME, Tall oil with a rich resin acid composition and Hexadecane.

#### 2.1. Fatty Acid Methyl Ester

Tall oil contains two distinguished types of chemical compound, namely FAME and resin acids with traces of neutral compounds.

FAME consists of an ester compound attached with a methyl group and a C<sub>17</sub> hydrocarbon with either a saturated (methyl stearate) or unsaturated (methyl oleate and/or methyl linoleate) carbon chain with traces of free fatty ester compounds (Paper III). For instance, the methyl oleate used as model compound in research as shown blow, contains the unsaturated C=C compound at C9 and C10 carbon.



The feedstock of the chemical compound FAME, which was received from SUNPINE AB, Piteå, was distilled from tall oil with 98% purities.

#### 2.2. Rosin Acids

Rosin acids comprise the mixture of resin acids and neutrals (Paper IV). Resin acids consist of an acidic compound (–COOH group) attached mainly to partially unsaturated polyaromatic

compounds with more than two rings. The main consequence of resin acids is the high melting point (above 25°C), which is a precipitated stage in blending with diesel. The feedstock of tall oil contains a mixture of FAME and resin acids.

**Table 2** Classified composition of resin acids with fatty acid methyl esters supplied by Preem AB (Paper IV).

Components	wt%	Components	wt%	Components	wt%
Octadecadienoic acid. C <sub>18</sub> :2	1.25	Isopimaric acid	1.37	b-Sitosterol	0.16
Octadecenoic acid. C <sub>18</sub> :1	0.80	Levopimaric acid	0.21	Squalene	0.34
Octadecanoic acid. C <sub>18</sub> :0	0.28	Palustric acid	1.32	Other	1.79
Methyl palmitate	2.82	Neoabietic acid	0.34		
Methyl linolenate	6.77	Dehydroabietic acid	4.45		
Methyl linoleate	35.75	Sandaracopimaric acid	0.42		
Methyl oleate	16.26	Pimaric acid	2.40		
Other esters	14.05	Abietic acid	8.69		
<b>Total free fatty acids and esters</b>	<b>78.41</b>	<b>Total resin acids</b>	<b>19.29</b>	<b>Total neutrals</b>	<b>2.29</b>

Moreover, different blends of rosin with light light gas oil (LLGO) are tested in our laboratory. The compositions of rosin blend in gas oil are shown in table 3:

**Table 3** Different blend composition of Tall oil with LLGO (PaperV)

Components	Mol. Weight	10% in LLGO	20% in LLGO	30% in LLGO
Free fatty acids	280 - 284	0.28	0.55	0.83
Fatty acid methyl esters	270 - 296	7.57	15.13	22.70
Resin acids	304	1.93	3.86	5.79
Neutrals	410 - 414	0.23	0.46	0.69

The tall oil feed material was supplied by Sunpine AB.

### 2.3. Rapeseed Oil

Rapeseed oil is rich in erucic acid and is the third largest oil source in the world after soybean and palm oil. It mainly grows in Western Europe, India, China and Canada [25-28]. The major constituent of vegetable oil is triglycerides. The properties of triglycerides and biodiesel fuel are determined by the amount of fatty acids present in their molecules. Two numbers designate fatty acids, with the first number showing the number of carbon atoms while the second number shows the number of double bonds. Different names of these fatty acids are given in Table 3.

**Table 3** Classified composition of rapeseed oil available in the market (Paper I and II).

Fatty acid content	Mol. Form.	Total (wt%)	C (wt%)	H (wt%)	O (wt%)
Free Fatty Acids (FFA)		0	-	-	-
Stearic (18:0)	$C_{18}H_{36}O_2$	7	5,4	0,9	0,8
Oleic (18:1)	$C_{18}H_{34}O_2$	61,1	46,9	7,4	7,0
Linoleic (18:2)	$C_{18}H_{32}O_2$	20,9	16,1	2,2	2,4
Linolenic (18:3)	$C_{18}H_{30}O_2$	9,1	7,0	0,9	1,0
Gadoleic (20:1)	$C_{20}H_{30}O_2$	1,4	1,2	0,1	0,2
Erucic (22:1)	$C_{22}H_{32}O_2$	0,5	0,5	0,1	0,1
Calculated (wt%)		100	77,0	11,6	11,4
Analysed (wt%)	Error = max.±0,5%		77,1	11,8	11,1

### 2.4. Light Light Gas Oil (LLGO)

Light gas oil is one form of a middle distillate product [29]. There are mainly four types of distillate. Light and middle distillates consist of kerosene and gas oil (automotive diesel), heating oil and general-purpose gas oil. Middle distillates generally refer to petroleum products in the boiling range beginning at above 160°C and ending at below 420°C, i.e. between gasoline and heavy fuel oil. LLGO is a part of the diesel fraction specially used for below cloud point (-40°C) in Scandinavian countries with a boiling point ranging from 160 to 320°C. This gas oil is supplied by Preem AB, Göteborg. The properties are listed in Table 4, which are used for the blend with FAME.

**Table 4:** Properties of LLGO supplied from Preem AB (Paper III, VI and V).

Properties	Value	unit
Aromatic content	17.8	% V/V
Cloud point	-40	°C
Density at 15°C	823.4	kg/m <sup>3</sup>
Dist: IBP	196	°C
Dist: Temp. at 10% V/V rec.	210.8	°C
Dist: Temp. at 50% V/V rec.	230.9	°C
Dist: Temp. at 90% V/V rec.	249.9	°C
Dist: Temp. at 95% V/V rec.	257.4	°C
Sulphur content	295	ppm (ppm)
Viscosity at 40°C	17773	mm <sup>2</sup> /s
Nitrogen content	< 1	ppm

### 2.5. Hexadecane

Hexadecane is an alkane type of hydrocarbon with the chemical formula C<sub>16</sub>H<sub>34</sub>. Hexadecane was purchased from Sigma-Aldrich with 98% purity and rest contains other alkane groups, that are blended with LLGO for isomerization feed material (Paper VI).

### 2.6. HDN-60 Catalyst

During the late 1970s, most of the N-heterocyclic model compounds were involved in the HDN (Hydrodenitrogenation) reaction by employing Mo or W oxide with or without a CoO or NiO promoter as a catalyst [30-34]. The incorporation of cobalt or nickel into the MoS<sub>2</sub> structure can significantly increase catalyst activity for hydrotreating reactions. Nickel atoms may be present in three forms after sulphidation: as Ni<sub>3</sub>S<sub>2</sub> crystallites on the support, as nickel atoms adsorbed on the edges of MoS<sub>2</sub> crystallites (the Ni—Mo—S phase) and as nickel cations at octahedral or tetrahedral sites in the  $\gamma$ -Al<sub>2</sub>O<sub>3</sub> lattice. Depending on the relative concentrations of nickel or cobalt and molybdenum and on the pre-treatment conditions, a sulphide catalyst may contain a relatively large amount of either Ni<sub>3</sub>O<sub>2</sub> or Co<sub>9</sub>S<sub>8</sub> or the Ni—Mo—S (or Co-Mo-S) phase [35-38]. However, the presence of H<sub>2</sub>S or organic sulphur compounds increases the rate of the removal of sulphur and promotes the rate of reduction.

Cobalt is mainly used in HDS, whereas Nickel is favorable for HDN. Ni atoms perform the real catalytic sites at Ni-Mo/Al<sub>2</sub>O<sub>3</sub> catalyst. MoS<sub>2</sub> acts as a secondary support for Ni atoms, in which MoS<sub>2</sub> crystalline in turn is supported by Al<sub>2</sub>O<sub>3</sub> [39-41]. Fully coordinated metal (Mo) atoms in sulfided catalysts will be unable to adsorb sulphur-containing molecules and thus the number of sulphur vacancies may be a key measure of the catalytic activity [42-49]. The binding energy of sulphur over the metal is the key role in catalytic activity in hydroprocessing. The activity was understood by sulphur bonding strength on catalyst, thus the density functional theory on Co/Ni-Mo-S type edges showed that both bonding and anti-bonding states are well below Fermi level, which promotes MoS<sub>2</sub> crystalline for desulphurization rate [50-53]. Even compared with other transition metals, these metals have much weaker sulphur bonding properties [54-59].

In addition, the catalytic pore size plays an important role in catalyst activities. Nakamura studied the preparation of a catalyst with 6% Ni and 18% Mo Oxides on various supported material with pore distribution and acidity [55]. The smaller pore size distribution gives better HDS activities than large pore catalyst. When tested with alumina-based supporting material, higher activities were observed for lower acidity [56-58].

### 2.7. Zeolite Catalyst

Zeolite is defined as a crystalline aluminosilicate with a three-dimensional framework that forms uniformly sized pores of molecular dimensions. Usually, acidic zeolite catalysts are used for hydroisomerization (e.g., Platinum on Al<sub>2</sub>O<sub>3</sub>, WO<sub>3</sub>/ZrO<sub>2</sub> and Platinum on Zeolite), such as differentiated according to composition of Si and Al ratio. Some of acidic catalyst used for isomerization are ZSM-5, ZSM-22, MCM-22, SAPO-11, H-Y (Mordenite), ultra stable Zeolite Y (USY), super dealuminated USY (SDUSY) and H-Beta types [60-65]. Zeolites are used as catalysts in research and commercial applications:

- ZSM-5 = Si/Al 20 to 50, high acidic
- ZSM-22 = Si/Al 80 to 90, low to moderate acidic
- H-Beta = Si/Al around 10, Complex structure zeolite
- H-Y = Si/Al around 6, (dealuminated)
- MCM-22 = Si/Al around 9 to 45
- SAPO-11 = Si/Al 0,01 to 4, presence of P (*Al = P wt basis*)

The special properties of zeolites are that they are strong and thermally stable, shape selective and non-corrosive. These special properties have allowed the zeolite to play an essential role in some processes for the conversion of a wide variety of hydrocarbons [66-75].



# CHAPTER 3

## Experiment Set-up

### 3. Experimental Methods

The experimental method consists of a reactor, analytical systems and distillation methods.

#### 3.1. Batch Reactor

The batch reactor consists of a gas inlet with two valves through which nitrogen and hydrogen gas are supplied to the reactor. There is a sample outlet connected to the gas inlet pipe with separate valves to control the flow. Further details of the batch reactor are given in Paper I and II.

The reactor is loaded with 150 ml of solution that includes a defined amount of catalyst and 3 g of tetradecane as internal standard. All experimental runs are conducted with stirring at a constant rate.

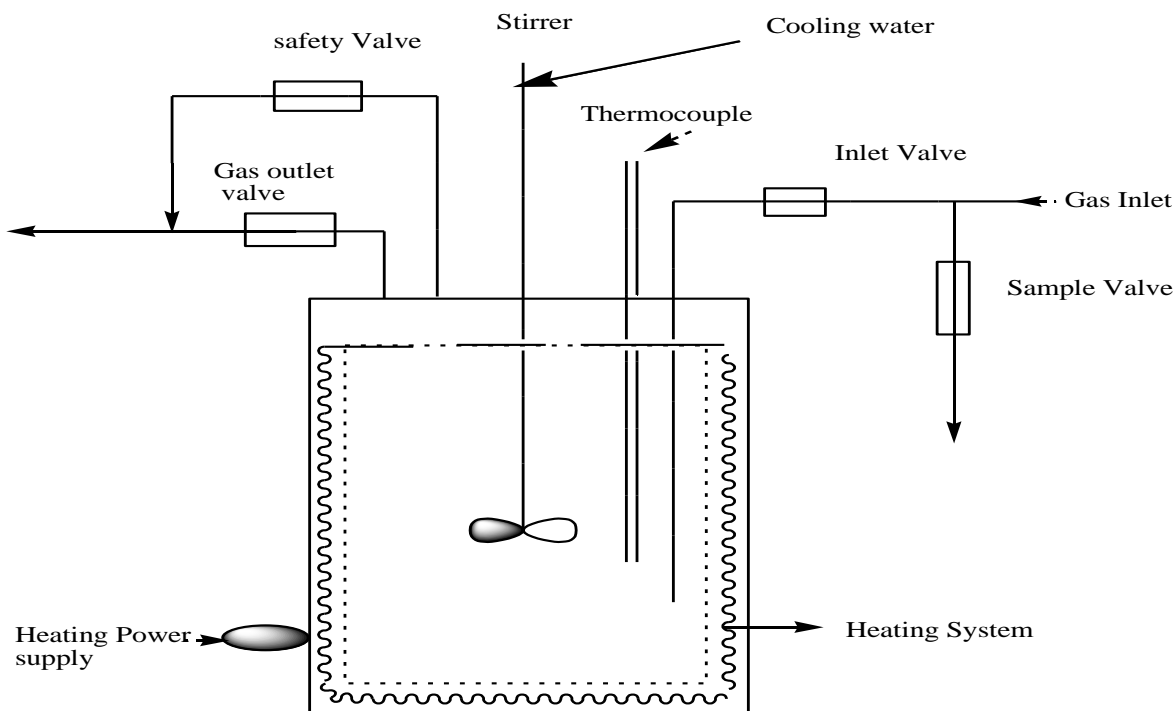


**Figure 1-** The main parts of an autoclave reactor and its application.

### 3.2. Fixed-bed Reactor

The experimental set-up consisted of a continuous reactor, feed and product tank, gas flow-meter, pump, gas chromatography and controllers. Brief description of reactor is explained in Paper I, II, IV and V. The reaction conditions were space velocity (ml/hr), reaction pressure ( $P_0$ ) (MPa) and temperature ( $T_0$ ) ( $^{\circ}\text{C}$ ). Overall reaction conditions were on a weight basis.

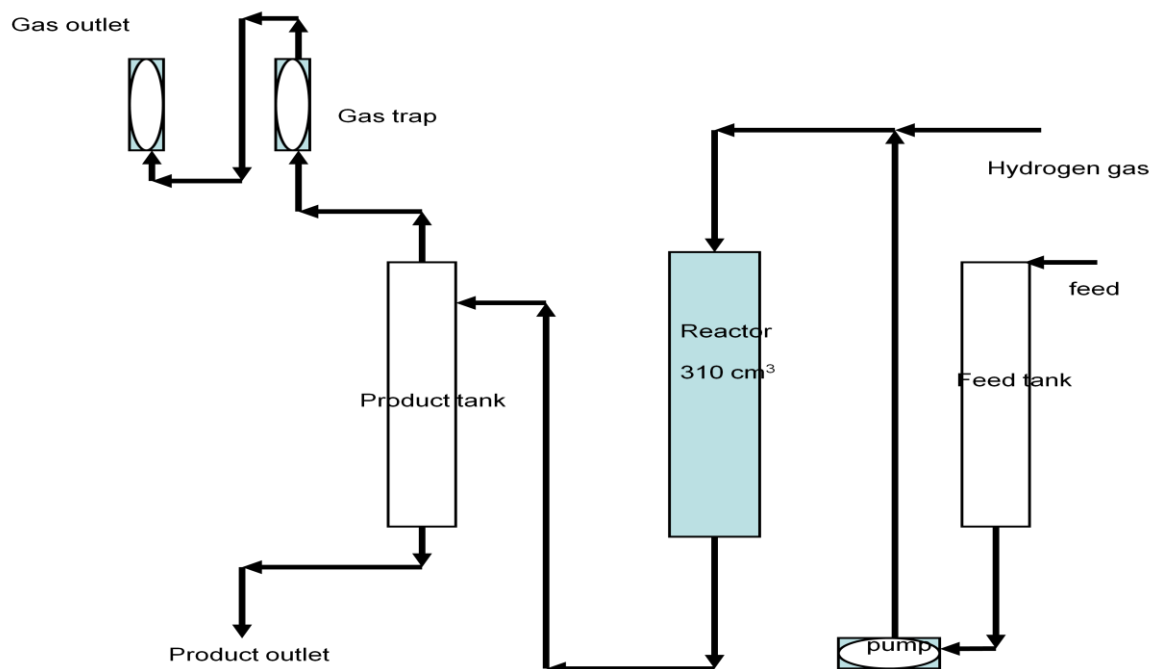


**Figure 2:** The main parts of a continuous fixed-bed reactor and its application.

The fixed-bed reactor was fixed with an electric furnace that was connected to an instrumental controller to regulate temperature and pressure. Further details about the fixed-bed reactor appear in Paper I, III & IV. The volume used for the catalyst was **31 ml** and the weight **27, 8561 g**. This volume is important to calculate space velocity (ml/ml.hr) with the following formula:

$$LHSV = \frac{\text{Volume product obtained}}{\text{time reaction of catalyst}}$$

### 3.3. Liquid Analytical Methods

The liquid products were analyzed using different gas chromatography equipment. Simulated distillation (ASTM D2887) was performed using a gas chromatograph (GC) (Varian 3400) equipped with a packed column (10% silicon OV-101, 80-100 mesh, 1m×1/8''×2.00mm) and a flame ionization detector (FID). The analysis was carried out at Chalmers University of

Technology (All the Papers) and the computation was made with an integrator Varian 4270. Samples (3 or 5µl) were injected into an injector through a micro-syringe. The analysis was done using the following settings:

Column temperature	325°C
Detector temperature	325°C
Initial temperature	40°C
Initial stabilizing time	2 min
Nitrogen pressure	6.2 bar
Hydrogen pressure	6.2 bar
Internal standard	n-Hexadecane
Rate	18°C / min
Final time hold	10 min
Sampling amount	6 µl
Injector – type	On-column

Elemental analysis of C, H and O was examined at Karlshamn Kraft AB. The ASTM D 5291 standard test method for instrumental determination of carbon, hydrogen and nitrogen in petroleum products and lubricants was used in our samples.

The liquid samples were analyzed with a Perkin–Elmer Spectrum One Fourier Transform Infrared Spectroscopy (FT-IR) to identify morphological changes by triglyceride (Paper I, II & III). Exercising extreme care, the samples were placed between two sodium chloride salt plates of high purity without air bubbles. The mid-infrared range

from 4000 to 400 cm<sup>-1</sup> was used to study the fundamental structure of the sample.

### 3.4. Gas Analytical Method

The outlet gas of the reactor was collected in a gas bottle and subsequently analyzed using the Clarus 500 online GC. A fuller description of the gas analysis is described in Paper I, II, III, IV and V. The settings for FID and TCD detector are shown in Table 5.

**Table 5:** Clarus 500 GC settings for TCD and FID detector.

Detector	TCD	FID
Initial temperature	40°C	60°C
Oven temperature	40 to 60°C	60°C
rate	8 °C/min	N/A
Initial holding time	8 min at 40°C	N/A
Final holding time	2 min at 60°C	15 min at 60°C
Carrier gas	Helium (6.2 bar)	H <sub>2</sub> (6.2 bar)
Sampling amount	5 µl	5 µl
Nitrogen pressure	6.2 bar	6.2 bar

### **3.5. Distillation Methods**

Hydroprocessed product contains lighter naphtha, gasoline and diesel fractions. To separate gasoline and lighter naphtha, simple distillation techniques is used. Aromatic content, Cloud point, S content, Density and Viscosity of diesel fraction were evaluated in Preem laboratory (Paper IV and V). The distillation column consists of a 2 L capacity re-boiler. It is heated to a desired temperature for removal of water and lighter fractions, which include naphtha and gasoline. The cut-off temperature is kept at 162°C for hydroprocessing of tall oil and 234°C for hydroprocessing of rapeseed oil, which is lower than normal distillation of diesel in order to avoid diesel fractions. The vapors are condensed through a water cooler. Lower hydrocarbons and water are collected in a distillate condenser after being cooled; any missing fractions are assumed to have escaped through the vent. After distillation, the product is kept under N<sub>2</sub> atmosphere.

### **3.6. Soxhlet Method**

Coke deposition on catalyst indicates the deactivation of active sites and pore plug. To identify coke, spent catalyst was analyzed in ASTM D5291 method (Paper IV). Before coke analyzes, spent catalyst should be free from solvent. The Soxhlet method has the purpose to wash the spent catalyst by using solvent depends on its polarity [78]. As the solvent boils, the vapor passes through the condenser, whereby the pure form of the solvent drops onto the sample to wash out undesired hydrocarbons on the spent catalyst. In our work, the spent catalyst NiMo/Al<sub>2</sub>O<sub>3</sub> is refined to extract the solvent by m-xylene for more than 22 hours in the Soxhlet apparatus. In a 250 ml beaker, 150 ml of m-xylene is loaded and heated to above 140°C. The vapor is passed through the soxhlet apparatus and cooled in a cooling tower. The spent catalyst is placed on a filter cover and washed continuously. Later, the refined catalyst is kept in a vacuum dryer above 125°C under nitrogen atmosphere for a day to remove the presence of m-xylene. The vacuum dryer is used to avoid loss of coke formation. The results from this procedure are discussed in Paper III & IV.

### **3.7. Characterization Techniques**

**N<sub>2</sub>-adsorption and BET surface area measurement:** The Brunauer, Emmet and Teller (BET) theory is the most popular model used to determine the surface area (results according to the Langmuir model are also available). Surface area measurement was provided by N<sub>2</sub>-adsorption according to the BET principle [30]. The concept of BET is an extension of the Langmuir theory with the hypotheses that gas molecules physically adsorb on a solid in layers

infinitely and there is no interaction between each adsorption layer. The BET surface area measurements were performed in a Micrometrics Surface Area and Porosity Analyzer (Tristar 3000) by adsorption of nitrogen. The samples were vacuum-dried at 523 K for 2 hours and cooled at room temperature prior to analysis. The results of the BET analyses for each catalyst are discussed in this section 3.6.3.

**Scanning Electron Microscope:** A scanning electron microscope (SEM) produces images of a sample by scanning it with a focused beam of electrons. The electrons interact with electrons in the sample, producing various signals that can be detected and that contain information about the sample's surface topography and composition. SEM can achieve resolution better than 1 nanometer. Specimens can be observed in high and low vacuum. In environmental SEM specimens can be observed under wet conditions.

### **3.8. *Hydroprocessing Catalyst- NiMo/Alumina***

The catalyst for the reaction is NiO-MoO<sub>3</sub>/Al<sub>2</sub>O<sub>3</sub> (Ketjenfine 840), which is commercially manufactured by Akzo Nobel. According to the manufacturer's specifications, the catalyst contains, in addition to the main components of NiO, MoO<sub>3</sub> and Al<sub>2</sub>O<sub>3</sub>, SiO<sub>2</sub> and traces of S, Na, Fe and others. The catalyst is crushed and grounded with a pestle in a porcelain mortar and screened on a stainless steel screen to a size ranging from 10-30 DIN mesh number (German Unit) whose aperture is equivalent to 0.2-0.6 mm. The catalyst is dried in air at 350°C overnight. The desired amount of the catalyst is noted and weighed without exposing for longer in air, this will avoid that moisture is absorbed on the catalyst. The catalyst is sulphidized at ambient pressure in a separate fixed bed up-flow reactor, which consists of a 25 mm diameter glass tube placed vertically in an electric furnace. Inside the glass tube the catalyst particles are placed on a glass wool supported on 2 mm diameter pearls that are kept in place by a stopper of glass wool. Gas is added from the bottom through a pipe inserted in a silicone rubber stopper at the bottom of the reactor. Through the silicone rubber stopper on the top of the reactor, there is a pipe for gas effluent and a thermocouple. A PID regulator controls the temperature. During activation, the catalyst is heated up to 400°C and the temperature is kept at this degree for 2 hours under a mixture of 10% by volume of H<sub>2</sub>S in H<sub>2</sub>. The catalyst is kept overnight under a N<sub>2</sub> flow.

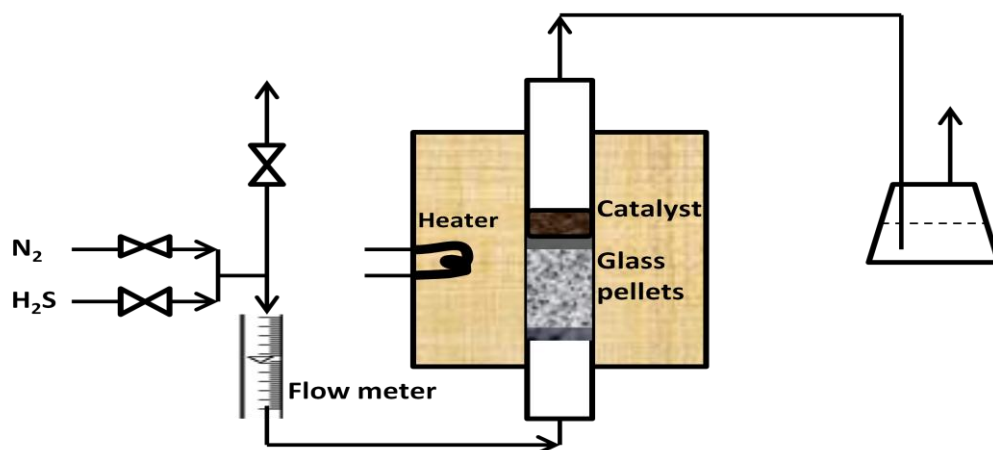


**Figure 3:** Sulfidation reactor and its main parts

Surface Area of the HDN-60 catalyst

BET surface area	189.7097 m <sup>2</sup> /g
Micropore area	7.3625 m <sup>2</sup> /g
External Surface area	182.3473 m <sup>2</sup> /g

Pore Volume of the HDN-60 catalyst

Single point adsorption total volume of pores less than 2067.018 Å dia.	0.3886 cm <sup>3</sup> /g
BJH Adsorption cumulative volume of pores between 20 and 3000 Å dia.	0.3857 cm <sup>3</sup> /g
BJH Desorption cumulative volume of pores between 20 and 3000 Å dia.	0.3961 cm <sup>3</sup> /g

### 3.9. Hydroisomerization Catalyst- H-beta Zeolite

The zeolite H-beta has been used as an acid catalyst in hydrocarbon conversion. The zeolite beta represented the high silica ratio with  $SiO_2/Al_2O_3$  between 10 and 200. The high-silica zeolite beta was first synthesized by Wadlinger and colleagues [79]. The synthesis was made from gel, organic template (tetraethyl ammonium cations) and alkali metal [80-89]. The zeolite beta has a potential acid sites, it is commonly recognized as high acid strength and hydrophobic thermal stability. Aromatic alkylation of biphenyl with propylene, aromatic nitration and aliphatic alkylation is a successful application of zeolite beta over the Friedel-Craft alkylation reaction [91-102].

The catalyst zeolite beta ( $SiO_2/Al_2O_3=360$ ) (with the trade name CP811C-300) was purchased from the Zeolyst International Company in Kansas, MO, USA. The zeolite (40 wt%) and  $\gamma-Al_2O_3$  (Disperal and Locron) (60 wt%) were mixed together and then extruded. The support material is dried at 110°C for 5 hours and then calcined at 350°C for 6 hours. After drying and

calcination, platinum was loaded with a Pt (NH<sub>3</sub>)<sub>4</sub>Cl<sub>2</sub> solution by ion exchange to get the content of 2.043 wt% Pt. The catalysts were dried at 110°C for 5 hours and calcined at 500°C for 4 hours in air (Paper VI). The pore size of extruded beta zeolite is depicted in Figure 4.

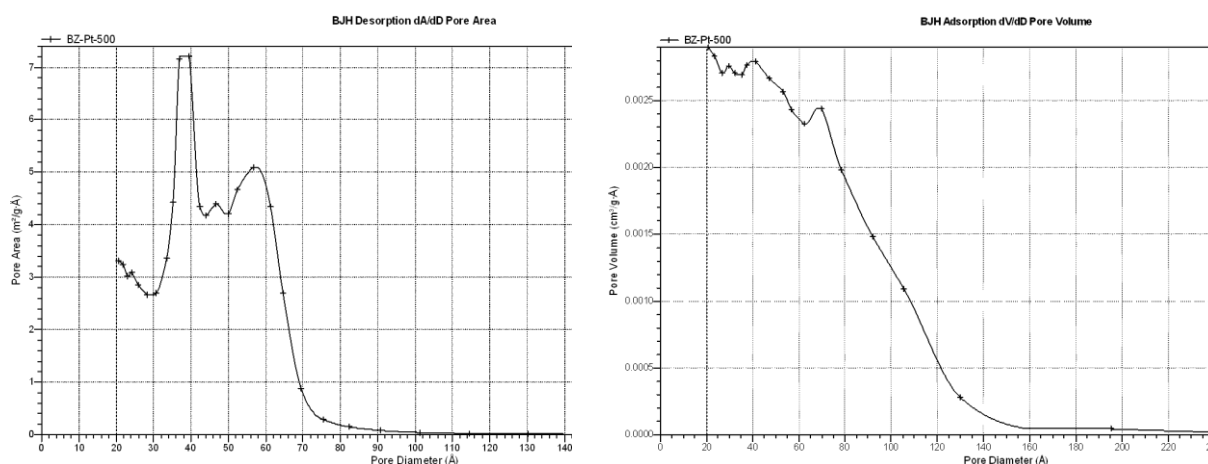


**Figure 4:** BET Physisorption characterization of extruded beta zeolite.

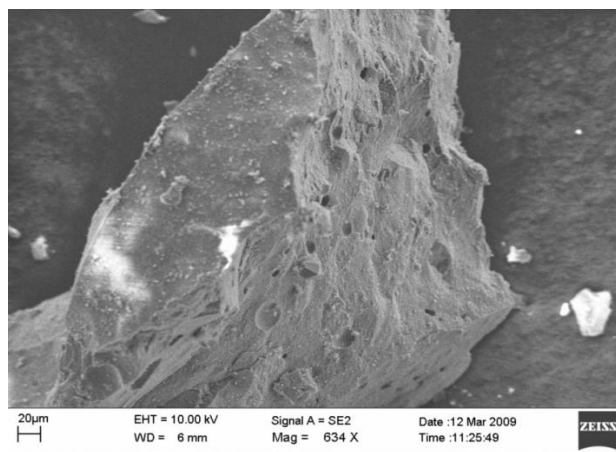
Figure 4 shows the pore area and pore volume vs pore diameter of the extruded catalyst. The  $\beta$ -zeolite contains large pore [49] with average pore width of 32 Å as measured by BET method and shown in Table 6. Extruded catalyst has average pore width of 41 Å.

Characterization	Surface Area (m <sup>2</sup> /g)	Micropore Area (m <sup>2</sup> /g)	External Surface Area (m <sup>2</sup> /g)	total pore volume	micropore volume (cm <sup>3</sup> /g)	average pore width (Å)	BJH Adsorption average pore diameter (Å)	Desorption average pore diameter (Å)
Molecular sieve	461.4	295.8	165.7	0.36	0.13	31.5	58.2	54.1
Extruder	248.4	87.5	160.8	0.25	0.03	40.8	51.4	46.3

**Table 6:** Characterization of zeolite molecular size and extruded catalyst

Depending on feedstock composition, presence of chlorine in zeolite enhances the octane number of the product [60-63,120]. Chlorine from Locron retained in catalyst pore. Quantitative estimate of Cl and Pt contents was carried out by the SEM techniques respectively. The composition of elemental metals presents over the section of catalyst is shown in Figure 5. The characterization results with absence of chlorine over the surface of the catalyst, but cross section of catalyst pellet has 0.34 mol% of total elements.

Spectrum identity	Wt %	Mol %
O	52.97	0.666
Al	32.99	0.244
Si	12.289	0.087
Pt	2.043	0.0025
Cl	0	0



Spectrum identity	Wt %	Mol %
O	49.31	63.71
Al	29.86	22.88
Si	17.35	12.77
Pt	2.09	0.307
Cl	0.58	0.338

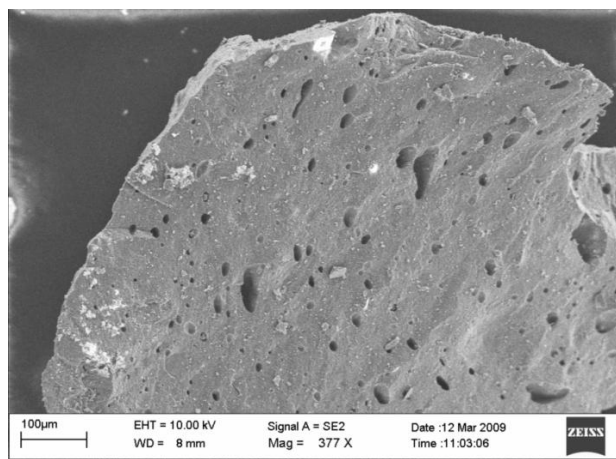


**Figure 5:** SEM characterization on the catalyst pellets: Elemental composition for top view and segmental view of the zeolite after extrusion and ion exchange techniques. Zeolite extruded morphological picture from SEM techniques. Two views of the zeolite are presented (top view and segmented view of the pellets).

### 3.10. Overview of the Experiments

The overall upgrading process of the tall or rapeseed oil is divided into three parts: thermal treatment, hydrodeoxygenation (HDO) and isomerization. The testing condition related to upgrading is as follows:

Process	Temperature (°C)	Pressure (bar)	Catalyst
Thermal treatment	250 - 390	1 & 50	no
Hydrodeoxygenation	300 - 390	40 - 70	NiMo/Al <sub>2</sub> O <sub>3</sub>
Isomerization	200 - 330	40 - 70	Pt/zeolite

The results are evaluated by the analytical study on different techniques as mentioned in Chapter 4. The addition of hydrogen using a particular temperature and/or pressure condition

leads to hydrogenate FAME into alkane that has a cetane number proportional to diesel. The hydrogenation of FAME might have different pathways, i.e. DCO, DCA and HDO. Indeed, except for DCO, the other two pathways need one or more mole ratio of hydrogen to sustain the desired product [8]. Contrary to the reaction of fatty acids, the exact route of catalysis with which the reaction is carried out is still unknown. A detailed analysis of each pathway is described below in relation to triglycerides hydrogenation.



# CHAPTER 4

## **Thermal treatment and decomposition**

### **4. Thermal Decomposition**

Refined rapeseed oil of 150 ml was placed in a batch reactor at 4.0 MPa partial pressure and 350°C for 3 hours with identical sampling time. Three experiments were conducted under the above-mentioned conditions: (1) with hydrogen and/or catalyst, (2) with hydrogen and without catalyst and 3) without hydrogen and catalyst, as mentioned in Table 7. All samples were analyzed by a FTIR and GC-FID analyzer.

**Table 7:** Thermal treatment test on Rapeseed oil under different conditions.

<b>Temperature Ranges</b>	<b>Conditions</b>
250°C, 275°C, 300°C, 325°C, 350°C	H <sub>2</sub> and catalyst
300°C, 325°C & 350°C	H <sub>2</sub> , no catalyst
300°C, 325°C & 350°C	no H <sub>2</sub> , no catalyst
300°C, 325°C & 350°C	Catalyst and no H <sub>2</sub> ,

Some of the main results are described below.

#### **4.1. Thermal Treatment**

The main aim of the study was to identify thermal cracking and any morphological changes in vegetable oil or FAME in a pre-heater. Rapeseed oil and Methyl Oleate are used as a model compound to identify the above objectives (Paper I). The uniform distribution of the GC results showed the thermal decomposition profile (see Figure 6 a & b). Paper I describes the details of radical reaction and decomposition effects in vegetable oil and FAME. Higher boiling point hydrocarbon between 330 and 370°C in figure 6 describes the carboxylic and aldehyde group. Here, the distillation recovery indicate the cracking of C-C and C-O is evident.

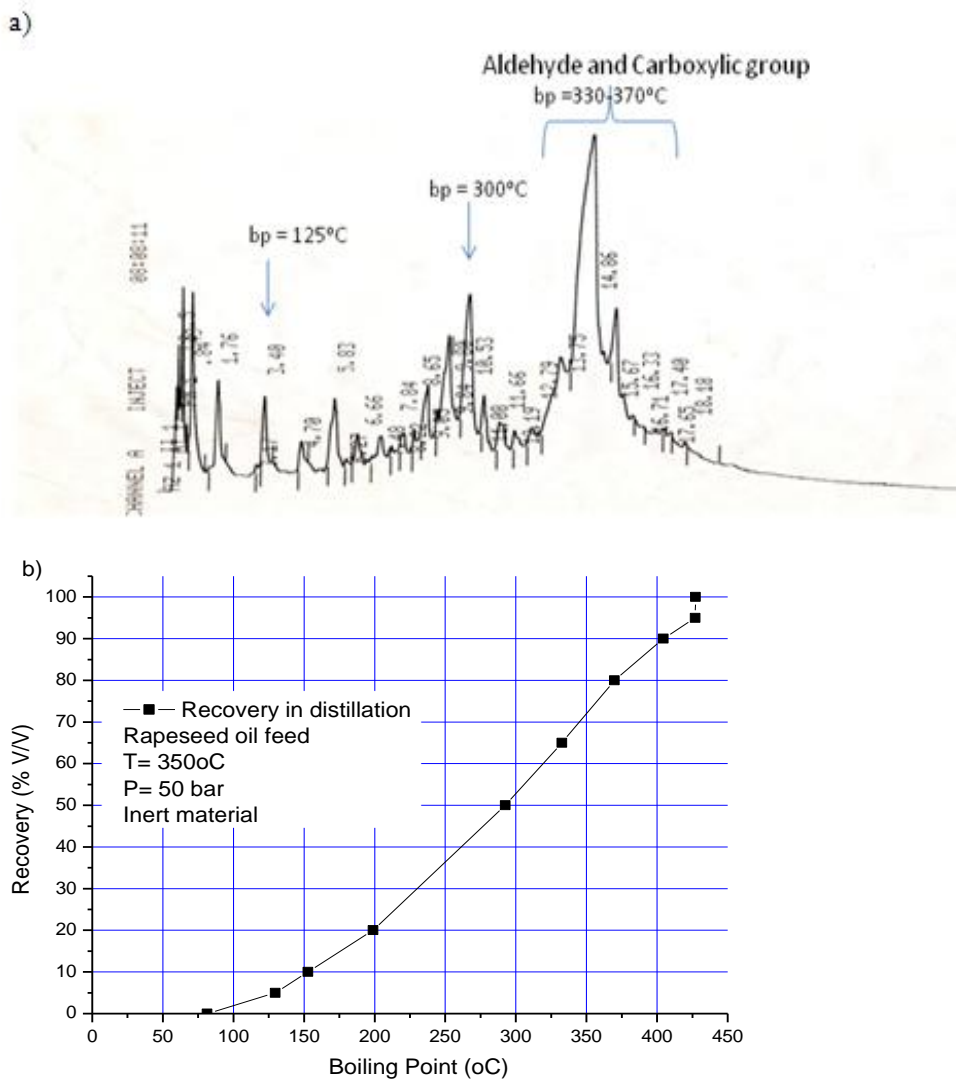


**Figure 6:** Hydrotreated vegetable oil at 350°C and 50 bar H<sub>2</sub> with glass pellets as inert material for 20 ml/min flow. (a) GC-SIMDIST analyses were done at Chalmers University of Technology. (b) Represents the recovery of the distilled product by laboratory test from Preem AB. note: bp=boiling point.

At moderate temperature between 330 and 370°C, C-C is evident for higher hydrocarbons range from 10 to 30 wt%. By the table 8 confirms that higher concentration of Oxygen content in distillates. Carbonyl compound influenced by temperature indicated in figure 6a, where large peak in GC appeared at boiling point 330 to 340°C. Between 330°C and 370°C, Oxygen content changes from 11.1 to 12.6 wt%.

**Table 8.** Rapeseed oil hydrotreatment at LHSV=20 mln/min, 1 bar and H<sub>2</sub>/oil=10. R-(C=O)O refers to Boiling Point from 340 to 360°C, R-(C=O) refers to Boiling Point about 330°C.

S. No.	Content	T (°C)	P (bar)	Recovered (wt%)	C (wt%)	H (wt%)	O (wt%)
R1	Rapeseed oil				77.1	11.8	11.1
VD2	Distillate	330	1	11.3	73.1	12	14.9
VB2	Bottom	330	1	88.7	80	12	8
VD1	Distillate	370	1	28.6	75.1	12.3	12.6
VB2	Bottom	370	1	71.4	80.9	12	7.1

The non-catalytic hydrotreated samples are analyzed with relative to C, H, O balances and presence of metal traces like N, Na, K and Mg are excluded. The results shows that moderate change in C and O composition were observed for moderate temperature between 330 to 370°C (Paper I). With cut-off T=230°C in distillation shows that higher composition of O in distillates than in reboiler. This indicates that C-O detachment in the glycerol group relatively sensitive to temperature (Table 8). This also confirmed for non-catalytic hydrotreatment of methyl oleate and dodeconic acids (Paper I). C-O detached weakly before C-C cracking; here, the radicals play a crucial role in the cracked alkyl group for further cracking of the same molecules (Paper I, II and III).

*Rapeseed oil treated at 350°C in a continuous flow reactor:*

The thermal decomposition in rapeseed oil is estimated with or without hydrogen at 1 and 50 bar partial pressure at 350°C. Initially, the reactor is loaded with glass pellets and heated up to 340°C and then feed material is fed at a controlled rate.

During the thermal condition of about 350°C on rapeseed oil, there are major interior glycerol structural changes and 15% of decomposition of the product group was evident (Paper I and II). The formation of the oxygenate group like aldehydes and ketones revealed to be 10 wt% in product concentration. In addition, the presence of a small amount of thermally cracked hydrocarbons was observed (Figure 7). The marked arrow in Figure 7 shows triglycerol structure modification, which shows changes in the position of carboxylic group and unsaturated C=C bonding in various radical reactions. Further, some cyclic group formation was observed. Detailed thermal decomposition is elaborated in Paper I and II.

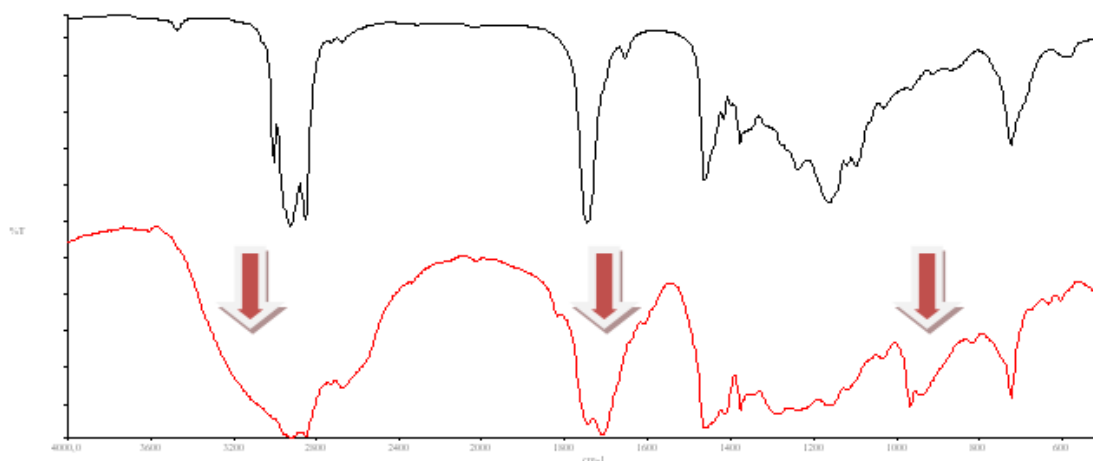


**Figure 7:** FTIR result of rapeseed oil treated without H<sub>2</sub> and with a catalyst at 350°C at 1 bar pressure.

The presence of the hexadecane and heptadecane groups at boiling point (280 to 305°C) was the major cracked product and a significant amount of carbon dioxide and carbon monoxide was seen in the outlet gas (Paper I). The general DCO and decarbonylation (DCA) reaction path was present in Figure 8, cracking and decomposition of carbonium groups described in paper I, II and III. Reaction mechanism of Thermal decomposition was described in Paper I, and the conclusion of paper I illustrated in schematic diagram at figure 8.

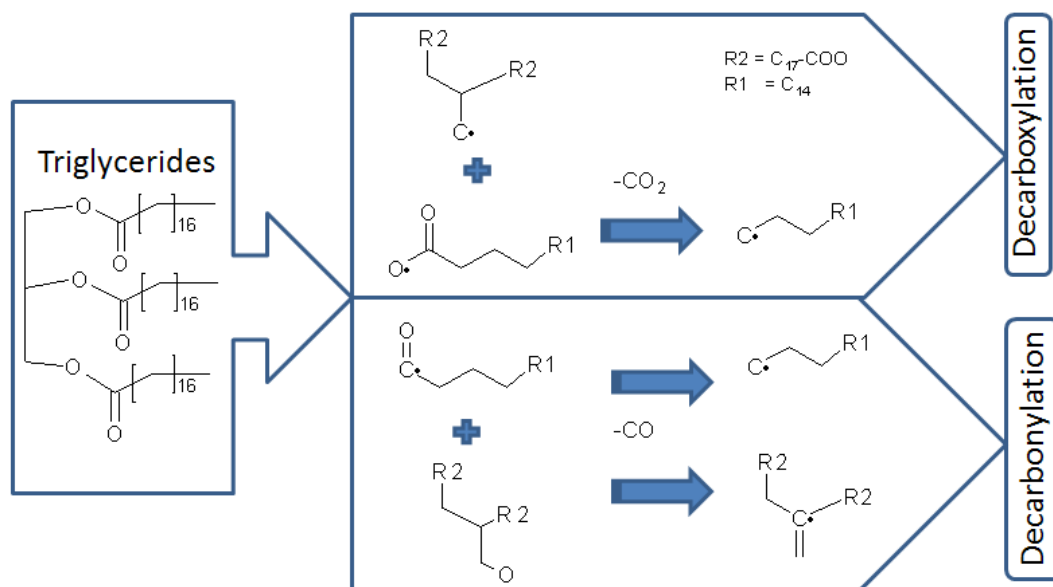


**Figure 8:** General formation of radical compounds from thermal treatment followed by decarboxylation and decarbonylation.

To analyze the thermal behavior of vegetable oil and related viscosity adjustment by cracking we studied different temperature adjustments for rapeseed oil in a batch reactor.

*Rapeseed oil treated without hydrogen and catalyst in batch reactor at 300 - 350°C:*

At 300°C, there is no shift in FTIR wavelength peaks as compared with feed and hence no significant change in the functional groups was evident. Thus higher temperature was examined. Figure 9 shows FTIR wavelength distribution for different period of sample for Rapeseed oil thermal treatment at 325°C. Formation of aldehyde group at IR absorption wavelength 2680  $\text{cm}^{-1}$  is observed. Decrease in the carboxylic group with longer residence time observed at wavelength 1700  $\text{cm}^{-1}$  indicated. For 325°C, the wavelength differs at 1300  $\text{cm}^{-1}$ , indicating a significant reduction of the ester group, also clearly can identify the thermal cracking at carboxylic group. Moreover, a peak at 1680  $\text{cm}^{-1}$  was observed with an increased concentration of the carboxylic group for longer residence time. Further description about 350°C results were discussed in Paper III.

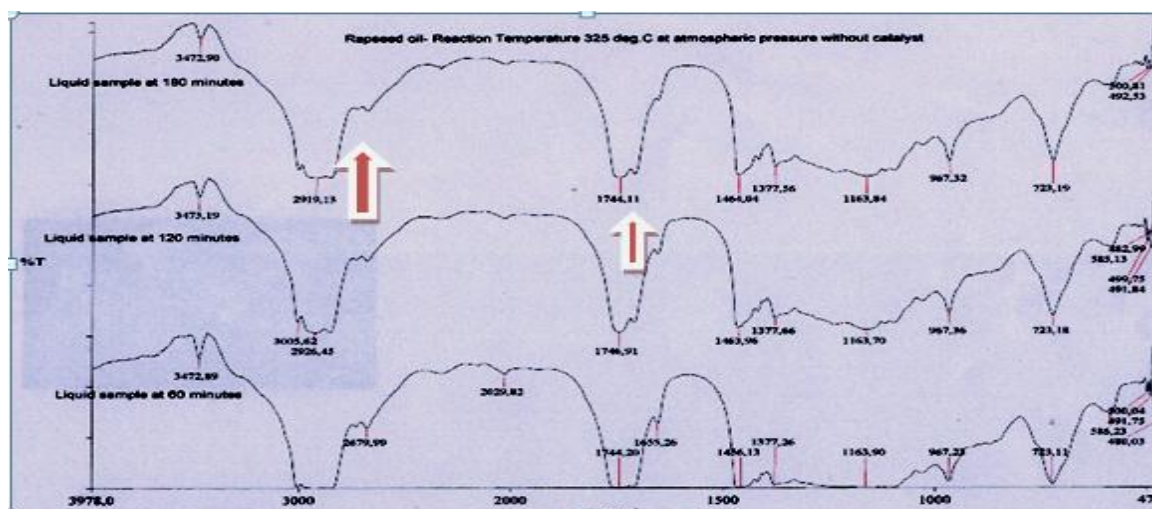


**Figure 9:** FTIR results of rapeseed oil treated without  $\text{H}_2$  and a catalyst at 325 °C at 1 bar. (Note: arrow simple shows the carbonyl group formation).

*Rapeseed oil treated with hydrogen and without a catalyst in batch reactor at 300 - 350°C.*

In this investigation hydrogen partial pressure was at a 50 bar throughout the experiment test. Temperature ranged from 325°C to 350°C. Figure 10 shows that there is a change in concentration of (OC)-O carboxylic group and presence of -OH functional groups from the fatty acids formed by decomposition. There is also restructure in the decomposed compounds due to hydrogen presence at high temperatures, which can be absorbed by a significant

reduction at 1750 to 1730  $\text{cm}^{-1}$ . Longer in contact time with inert material at higher temperature, changes in morphology of glyceride compounds was observed (Paper III). Decrease in aldehyde group for higher temperature at IR absorption wavelength 2680  $\text{cm}^{-1}$  was observed. Thus, there were major changes in the  $-\text{OH}$  group and  $\text{C}=\text{O}$  group of free fatty acids, which were identified with H-abstraction and  $\text{C}=\text{O}$  stability (Paper I, II, and III). However, the experiment with the batch reactor demonstrated only carboxylic group behavior with residence time in moderate temperature (Paper III).

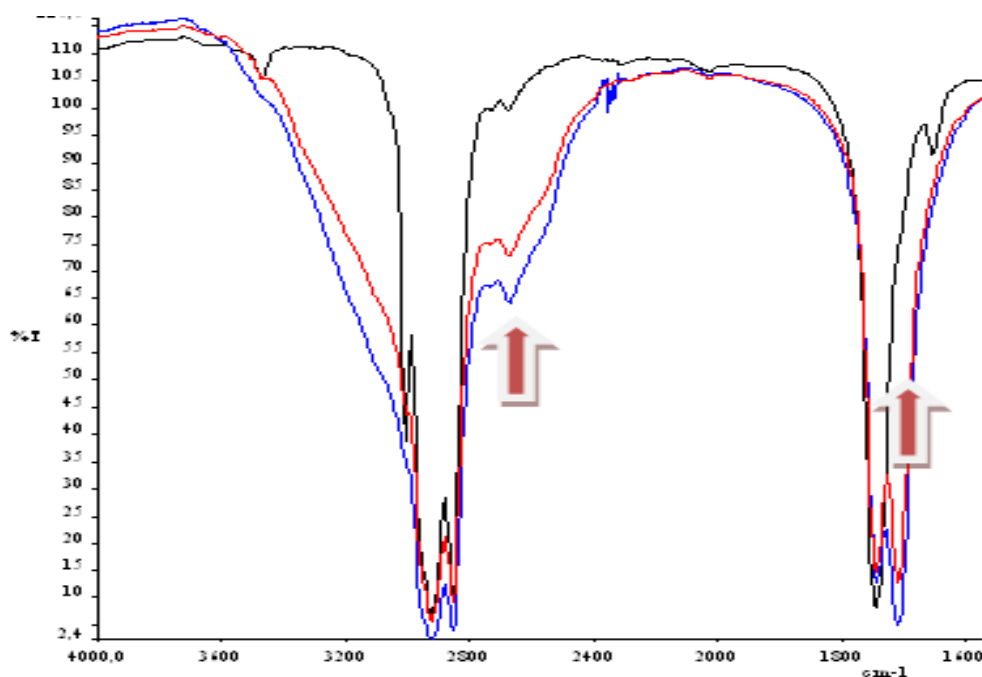


**Figure 10:** FTIR result of rapeseed oil treated with  $\text{H}_2$  and without a catalyst at  $350^\circ\text{C}$  at 40 and 80 bar pressure. (Note: blue line - at  $350^\circ\text{C}$  and red line - at  $325^\circ\text{C}$ ). (Note: arrow simple shows the carbonyl group formation).

#### 4.2. Thermal Decomposition

The study of FTIR measurement was performed in order to analyze the C-O and C-C bond breakage for triglycerides, particularly temperatures between 300 and  $370^\circ\text{C}$ . This study was done to understand the carbonyl thermal cracking. Thermal impact over the ether-chain affects the methyl group and hydrocarbon chain due to C-O detachment (Paper I, II and III). The results showed there was an increase in peak at a wavelength between 2500 and 2800  $\text{cm}^{-1}$ , indicating the  $\text{CH}_X$  group of the fatty ester group (Paper I and III). Peak wavelength at 1710  $\text{cm}^{-1}$  showed the formation of carboxyl acids that was due to  $\alpha$ -carbon bond breakage (Paper III). Here, the C-O bond of  $\alpha$ -carbon broke at low enthalpy by leaving  $-(\text{C}=\text{O})^*$  as residue, where the presence of either aldehyde or acid from decomposition effect was observed. The

strength of hybridized indicated the C-H bond stretch [74]. In general, higher concentration at  $3100\text{ cm}^{-1}$  indicates for the  $\text{sp}^2$  carbon and  $2900\text{cm}^{-1}$  indicates for the  $\text{sp}^3$  carbon. Here,  $\text{sp}^3$  hybridized C-H bond need lower energy than  $\text{sp}^2$  carbon for stretching. Increase in temperature induce  $\text{sp}^3$  hybridized C-H bond cracking and it is also applicable for free fatty acids cracking. When the proton removed from the carbon in carbonyl group involve a delocalized electron to oxygen for stability. Here, oxygen is at high reactive state. By the presence of catalyst and hydrogen, the basic character of oxygen from delocalized carbonyl group increase the rate of reaction. Also, similar rate of the reaction is induced in glycerol group which has delocalized oxygen. The proton transfer from  $\beta$ -carbon, i.e., transfer of H atoms by abstraction, can form  $-\text{OH}$  group which can be seen at wavelength  $3450\text{ cm}^{-1}$ . Increase in carboxylic group was observed in the sample for long residence time in the reactor. This leads to the formation of free fatty acids and di-glycerol groups. There is a significant change in the ester group due to high temperature and residence time, which tends to break the  $\sigma$ - bond rather than the  $\pi$ -bonds.



# CHAPTER 5

## **Catalytic hydroprocessing technique**

### **5. Catalytic Hydrotreating Process**

Today, Pd, Co and Ni are the most frequently used metals for catalytic hydroprocessing in refineries. Pd catalysts are highly active in the hydrogenation of double and triple C-C bonds but much less active in the hydrogenation of aromatic hydrocarbons and C=O bonds. Ni- or Co-based catalysts, often named HDN catalysts, are widely popular in hydroprocessing techniques. Detailed study of research work on catalytic hydro-treatment is presented in Paper IV and V, respectively. Relative in carbonyl group hydrogenation and gas oil fraction cracking has studied with few researches [48-49]. Gas oil blending with FAME results in removing sulphur from middle distillates. Here, we focused mainly on properties such as Sulphur, aromatic group, catalyst activity and Product selectivity.

#### ***5.1. Fatty Acid Methyl Ester Hydroprocessing***

The sulphur content was generally less than 10 ppmw in the upgraded product. Initially, few samples were observed to be near 25 ppmw S, a condition that might be because either activation of the catalyst with hydrogen sulfide was not complete or coke deposition over active sites reduces S-bond strength in optimum fermic energy to enhance the active sites. After periodic experimental samples, sulphur was less than 10 ppmw, which explains that the activity was increased on the catalyst through coke deposition in spent catalyst. The continuous addition of sulphur on vacant sites significantly lowered the deactivation of the catalyst. Formation of coke over the catalyst lead to neither incline increase in sulphur slip in catalytic bed or decline in activity of desulphurization was observed. It also determined that the pore clogged with coke has less impact in the selectivity of products. Selectivity of C<sub>18</sub>/C<sub>17</sub> was moderately increased during the testing period (Paper IV). Initial coke depositions on the catalyst induced an advantageous effect for sulphur removal. At 350°C, the presence of the aromatic group in the upgrade product had a similar grade as feed. An increase in temperature resulted in an increase in the aromatic group. This increase in the

aromatic group indicates that the carbonium ions from cracking induced the radical group interaction in the same carbon chain. In addition, saturation of carbonium ions by abstraction of hydrogen from the same chain is possible. However, this is rate limited due to space velocity and availability of active sites (Paper IV). The overall reaction mechanism illustrates that the yield of carbon from FAME is achieved over a long-term catalyst life.

## **5.2. Rosin Acids Hydroprocessing**

The results show that although the resin acid is transformed into lighter components, the product comprises aromatics and some heavy components that are unsuitable as additives to diesel fuel.

High C<sub>18</sub> formation is favored at lower thermal conditions (i.e. about 330°C), whereas low sulphur outlet and better reaction stability result from low cracking. Concerning the cloud point factor, there is a higher point as compared with a higher thermal condition. However, this observation is only evident for the 10% FAME mixture; for the 30% FAME mixture, the cloud point is almost the same, regardless of thermal condition. Furthermore, in gas outlet, higher CO<sub>2</sub> outlet and low CH<sub>4</sub> are disappointing factors. In case of CO, there are almost no changes in relation to thermal condition. Resin acid decomposition is low at 330°C. At a higher temperature (i.e. about 360 °C), higher C<sub>17</sub> formation is favored, but high cracking and higher sulphur content (3 – 4 ppm increase) are not good signs with respect to practical application (Paper V). For a lower cloud point, a higher thermal condition might be utilized during the winter period. These are good conditions for C<sub>19</sub> and C<sub>20</sub> compounds to crack.

Aromatic content and PAH increase proportionally with an increase in the thermal condition. Here, a 50-bar pressure condition is not sufficient in reducing aromatic content from the inlet concentration. However, it is possible to maintain the same level at lower thermal conditions. In case of high FAME blend, an increase in aromatic content indicates there is low cracking of rings from resin acids. Therefore, to achieve maximal diesel quality, a lower FAME blend of about 20% is recommended.

The hydroprocessed abietic acid results with increase in 50% aromatic compounds, out of which 85% of aromatic compounds are mono-aromatic group (Paper V). The reaction pathway diagram of abietic acids hydrogenation from our research prediction is displayed in Figure 11.

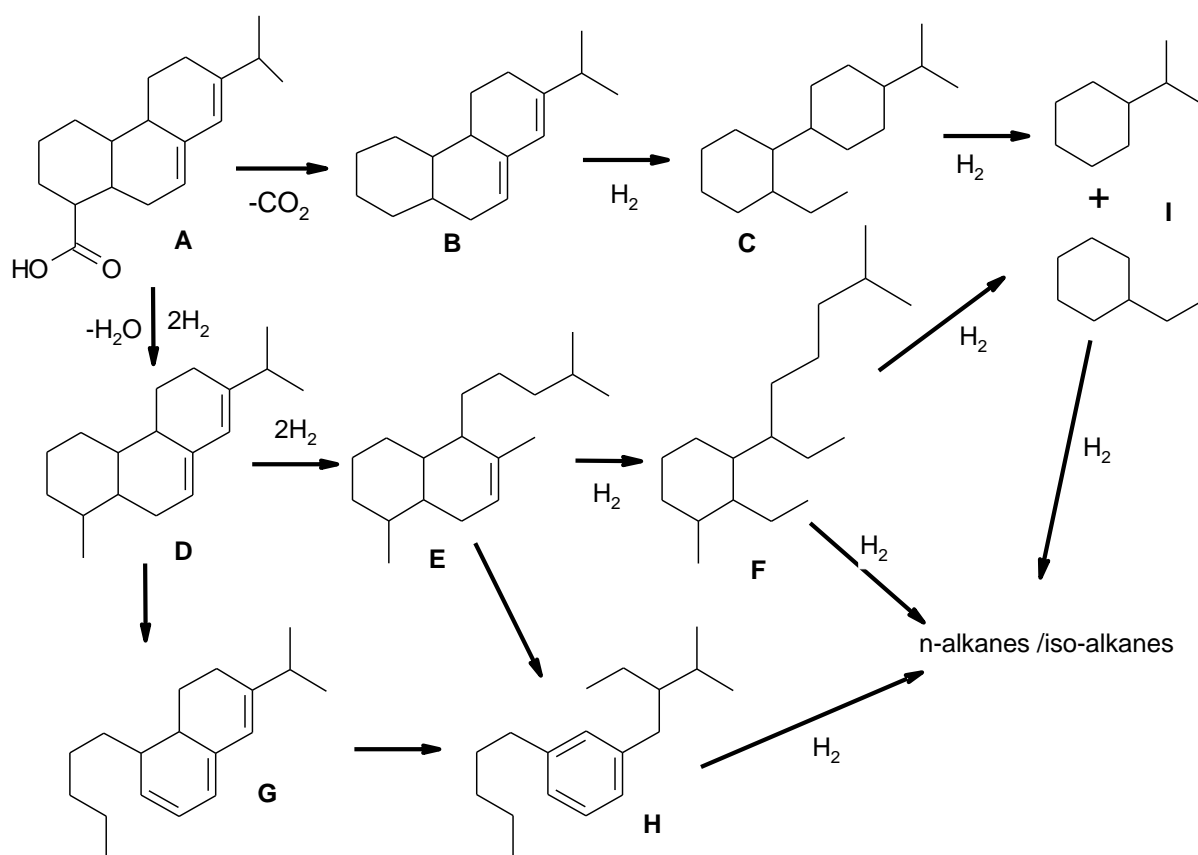


**Figure 11:** Abietic acid (A) hydro de-oxygenation reaction at 350°C and 50 bar H<sub>2</sub>. (Note: reaction mechanism was drawn by Paper V results and discussion).

### 5.3. CO and CO<sub>2</sub> in Fuel Gas

Temperature and space velocity affected the results of the gas analysis. For this analysis, the gas collector must be heated before injecting the gas sample into the chromatograph. This rise of temperature inside the small collector increases the pressure, which is necessary to achieve a correct analysis of the important components of the experiment. It should be emphasized that the entire gas product obtained is produced by the cracking of the original product. This is because the feed is liquid. Analyzing percentage of volume shows that the component most often produced in almost all the cases is methane (CH<sub>4</sub>). This is due to the three reactions that occur at the reactor: DCA, DCO and hydrodeoxygenation (Paper IV and V). In all three reactions, one of the products of the reaction is methane, and its amount rises as the temperature increases, except in the case of 1.2 LHSV, which might be attributable to an experimental mistake in the analyses because it was quite sensitive to the temperature of the collector before the injection of the sample.

The relative rates of the DCA versus DCO pathway can be compared by looking at the CO and CO<sub>2</sub> yields. These two yields are relatively equal; both increase by approximately the same value with increasing temperature. These results indicate that the rates of these two reactions are similar and that the same underlying mechanism is involved in the reactions.

The first step is CO<sub>2</sub> dissociation into surface CO and O (CO<sub>2</sub> → CO + O) and the sequential dissociation of CH<sub>4</sub> into surface CH and H (CH<sub>4</sub> → CH<sub>3</sub> → CH<sub>2</sub> → CH). The second step is CH oxygenation into CHO (CH + O → CHO), which is more favored than its dissociation into C and hydrogen (CH → C + H). The third step is the dissociation of CHO into surface CO and H (CHO → CO + H). Finally, H<sub>2</sub> and CO desorbs from Ni(1 1 1) to form free H<sub>2</sub> and CO. The rate-determining step is the CH<sub>4</sub> dissociative adsorption while the key intermediate is surface adsorbed CH-O. Parameters that might modify the proposed mechanism have been analyzed. In addition, the formation, deposition and elimination of surface carbon have been discussed accordingly (Paper IV and V).

#### 5.4. Decarboxylation and Decarbonylation

Rapeseed oil was hydrogenated in a batch reactor under 300 - 350°C and 40-100 bar pressure. Through hydroprocessing, the carboxylic group of rapeseed oil changes morphology and leads to cracking of the C-O group.

The parental fatty acid loss one mole C as CO and dehydration with limited hydrogen intake which gives C<sub>n-1</sub> compounds is called decarbonylation (DCO). The decarboxylation (DCA) path represents the removal of CO<sub>2</sub> from the carboxylic group. Removal of the Carboxyl group can be observed through HDN catalysis, but this might be limited because of a side reaction in the hydrogenation process. Thus, to reduce the loss of Carbon as CO /CO<sub>2</sub> by DCO/DCA, a more controlled reaction condition with in-depth analysis and experimental work is needed (Figure 12). There might be an equal amount of cracking in hydrocarbon C<sub>4</sub> to C<sub>12</sub> and a high-pressure condition suppresses the C-C cracking from the complex structured ester group.

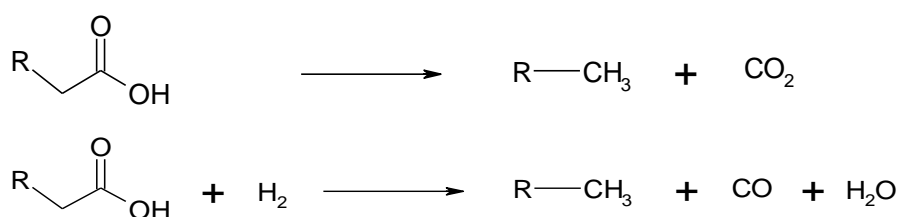


**Figure 12:** Decarboxylation and Decarbonylation of fatty acids

Poulloux et al, who hydrogenated methyl oleate with Co-Sn/Al<sub>2</sub>O<sub>3</sub>, showed stearyl alcohol (also known as octadecyl alcohol or 1-octadecanol) is a major product at 270 °C and 8 Mpa pressure. Lately, Senol et al proved the DCO by methyl heptanoate is achieved with sulphided Co or Ni -Mo/Al<sub>2</sub>O<sub>3</sub> catalyst at 250°C and 8 Mpa pressure, but formation of esters reduces the conversion efficiency. Here, these carbonyl reductions are mainly achieved by Lewis acid site. Croma et al confirm that the conversion by DCO and DCA has the same proportion by Ni-Mo/Al<sub>2</sub>O<sub>3</sub> [16]. Murzin et al research on decarboxy/decarbonyl with Pd/C catalyst gives maximum of 55 mol% conversion of heptadecane from stearic acid at 300°C [105, 110]. From the extensive studies prevailed to understand that DCO in FAME and vegetable oil depends on temperature and hydrogen demand to overcome barrier on interfacial mass transfer resistance on catalytic surface.

We have studied rapeseed oil hydroprocessing with sulphide NiMo/Al<sub>2</sub>O<sub>3</sub> in a batch reactor. Formation of a carboxylic group was slow and the rate was limited with residence time (Paper III). A longer residence time resulted in a steady increase of an oxygenated group, but deactivation of a catalyst results in a loss of S, which significantly lowers the product formation.

The hydroprocess needs an excess amount of hydrogen, which yields water as an undesired product. In particular, hydroprocessing FAME with a blended diesel in commercial use with NiMo/Al<sub>2</sub>O<sub>3</sub> helps to reduce sulphur content. Research is currently being done with vegetable oil blended in diesel-desired hydrodeoxygenation (HDO) than DCO and DCA.

### ***5.5. Deoxygenation and Desulphurization***

In general, removal of organosulphur has two routes: a one-step process of direct desulphurization or a two-step process of desulphurization and separation techniques. The process of removing oxygen with CO<sub>2</sub> and H<sub>2</sub>O from the carboxylic group in presence of hydrogen to get a hydrocarbon aliphatic compound is called HDO, one-step desulphurization technique. For HDO, search for a catalyst, optimal temperature and pressure conditions is in progress in order to achieve a better diesel product. Hark et al revealed that hydrogenation of FAME under a super critical condition is effective to give fatty alcohol under Cu catalyst [119]. The hydrogenation of lipids in FAME (Fatty acid methyl ester) in continuous reactor with the presence hydrogenation at 240-250°C and 150 bar pressure gives favorable result. Indeed, this is the main motivation to remove oxygen from aliphatic hydrocarbon compounds (such as FAME). Despite Cu, recent studies have shown that sulphide hydrotreating catalysts

(e.g., NiMo and CoMo/Al<sub>2</sub>O<sub>3</sub>) produce better conversion. From this work, the Co-Mo HDS catalyst showed good contribution. In phenol and anisole hydrogenation Viljava et al identified better reaction stability of the HDS catalyst in the presence of H<sub>2</sub>S, does not affect the selectivity [73]. HDO conversion reached 72% at 300°C, but the formation of the final product is still not optimal. Senol et al found that Co & Ni-Mo/Al<sub>2</sub>O<sub>3</sub> with H<sub>2</sub>S and water with feed increases ester level [75-77]. However, the addition of H<sub>2</sub>S effectively compensated the inhibition by water. Furthermore, the authors noted that the Ni catalyst has better activity and stability than Co. Senol et al recommend H<sub>2</sub>S as promoting sulphiding agent with attributed to acid-catalyzed reaction [77,118]. The result of methyl heptanoate hydrogenation through HDO mechanism provides C<sub>7</sub> and C<sub>6</sub> aliphatic compounds. Here E<sub>2</sub> elimination and SN<sub>2</sub> nucleophilic substitution mechanism as proposed reaction role. From this background, we have started to investigate FAME and tall oil hydroprocessing with gas oil blend. The estimated reaction mechanism of FAME hydroprocessing in figure 13 shows dehydration and carboxylation has similar rate determination, while esterification involves the rate determination. Above 350°C, decomposition of esterifies compound favored towards decarboxylation and below 350°C, esterifies compound favored towards deoxygenation.

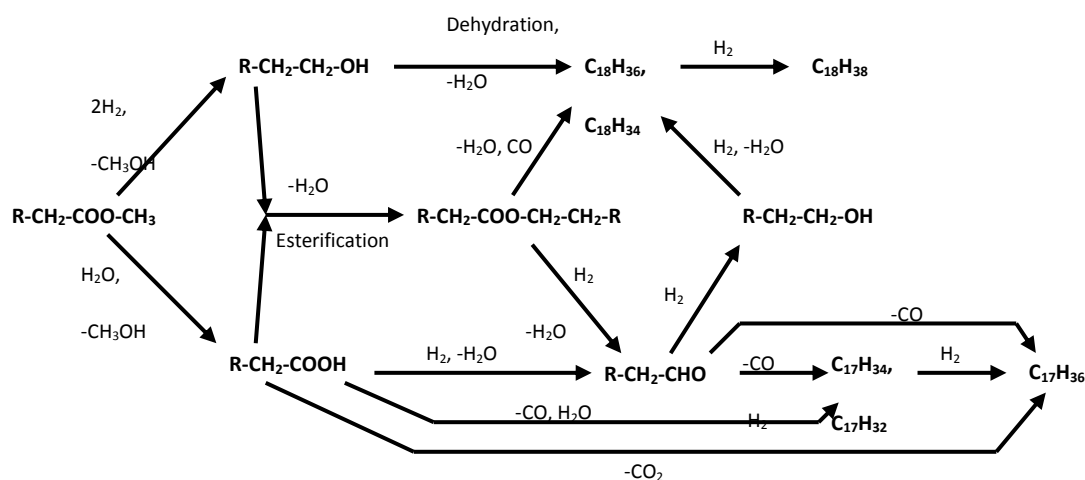


**Figure 13.** Estimated reaction mechanism of Hydrodeoxygenation of fatty acids from our results.

Subject to HDO mechanism, results are mainly evaluated with different space velocities and temperatures parameters in pilot study. However, partial pressure adjustment directly influences by reducing appearance of naphtha and cracking. Variation of space velocity and temperature is shown in Figure 14. Higher temperatures and lower space velocities are inclined to give cracking, and vice versa, respectively.

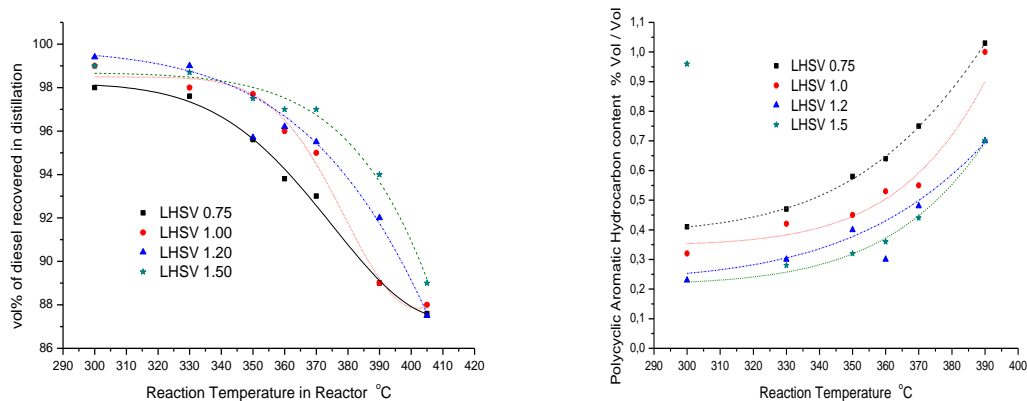


**Figure 14.** Hydrodeoxygenation of FAME blend with LLGO

Gas oil consists of straight-chain and poly-aromatic hydrocarbon (PAH) with traces of heteroatom (e.g., Ni, V, Na, N and O). The presence of S in gas oil is usual in the range of 300 to 2000 ppm. This can be achieved by breaking lower bond energy of C-S, i.e. 255 kJ/mol, and retain the yield with low cracking of C-C (347 kJ/mol) [90]. Here, research has mainly focused on checking the yield of the exothermic reaction by substituting H-donor. In some cases, presence of methyl group or ethyl group due to a steric hindrance effect by adjacent C-S bond increase kinetic rate of reaction. Thus, high partial pressure is required with moderate temperature to break the bond. Even the use of a different technique (such as microwave or ultrasound radiation) can minimize resistance. Figure 14 shows increase in PAH with temperature and space velocity. Sulphur presence in cyclic group or straight chain of distillates abstract H atom from catalytic sites to form H<sub>2</sub>S. Straight chain hydrocarbon with sulphur undergoes faster rate of desulphurization compared to cyclic group. Larger cyclic group over position of bonding in catalyst had difficult to abstract H-donor from neighbor site, so abstraction of H from  $\beta$ -position might involve an electron deficiency over carbon. Delocalization of proton takes place within the cyclic group. As the delocalized proton retain in cyclic group with deficiency of electron. This electron deficiency has similar impact for C-C bond detachment. Increase in residence time, as shown lower space velocity test in figure 14, has tendency to give higher PAH and lower diesel grade. For lower contact time, the result shows same in feed and product for aromatic content and gasoline fraction.



# CHAPTER 6

## **n-Paraffinic Upgrading**

### **6. n-Paraffin Upgrading Process**

Enhancing octane number (RON) through isomerization of C<sub>4</sub>-C<sub>6</sub> n-alkanes in gasoline is commercially available in many refineries. Isomerization of higher naphtha and paraffin hydrocarbon groups for Fischer-Tropsch products have been studied with different zeolite [60]. The skeletal rearrangement of n-paraffin mainly depends on the acidic nature of the catalyst, the transition metal distribution on the support material, the surface area of the catalyst and the partial pressure of hydrogen. The catalyst of low acidic and high hydrogenation activity has a greater influence on isomerization than hydrocracking [51, 60-62]. Isomerization of alkanes in petroleum industries is to enhancement properties such as cloud point, pour point, viscosity, density and combustion. On most of these cases, the fine product is manufactured through a zeolite catalyst (e.g., SAPO, ZSM, H-beta, Y-type and AlPO<sub>4</sub>), discussed more in section 2.7. These zeolite catalysts have recently become more popular because of their diverged application in hydroprocessing industries. Selection of β-H zeolite with high Si content has advantage of thermal stability, selectivity and activity, also, larger concentration of bridging –OH with Al and Si. Consequences of proton donor from Si-H influence isomeric compounds rather than cracking [122].

#### **6.1. Thermal-Cracking**

Hydroisomerization works to reduce cold properties of fuels. Temperature and catalytic structure are vital properties that mainly depend on branching alkanes. We mainly use acidic catalyst-like β-zeolite under moderate temperature conditions (210 – 270°C). One such condition with a space velocity of 1 at 50 bar H<sub>2</sub> total pressure is presented in figure 15. The sample contains cracked naphtha and branched alkane's which preferably influence the product yield and selectivity. Hydrocracking in isomerization is unavoided side reaction. The temperature influence on cracking has a direct effect to break the C-C bond. However, the acidity of the catalyst has a major influence on the hydroisomerization and hydrocracking mechanisms. More discussion about hydrocracking is available in Paper VI.

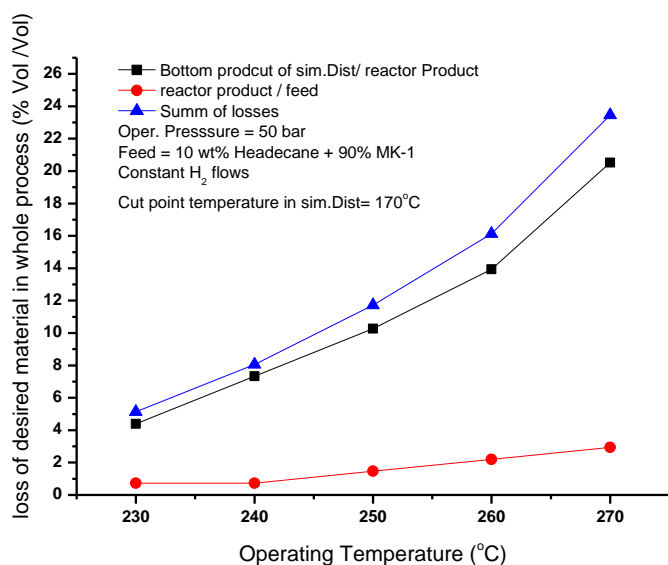


**Figure 15.** Hydroisomerization recovery of diesel in an experiment with a space velocity of 1 and 50 bar H<sub>2</sub> total pressure

## 6.2. Hydroisomerization

Generally, the Friedel-Craft catalyst has high activity on lower temperature conditions which degraded from commercial application due to corrosion and product loss. However, the usage of transition metals as a catalyst, which performs to provide better selectivity and catalyst life compared with a Friedel-Craft catalyst, operates under higher temperatures and shows dual-functional activity (hydrogenation-dehydrogenation).

Isomerization of 10-wt% hexadecane is blended in gas oil and tested with beta-zeolite. Figure 16 shows the conversion of C<sub>16</sub> which reaches 100% at 270°C. With the selectivity graph in Paper VI shows that the reaction attained equilibrium at 250°C, with only 10 wt% loss as naphtha in cracking and appearance of isomeric alkyl composition at peak on bi-functional catalytic activity. To determining the reactivity and selectivity of this catalyst, different space velocity experimentation at 240°C was tested. Boiling point range between 260 and 281°C increases linearly with space velocity which implies in isomeric compound formation (Paper VI). Catalysts with a high degree of hydrogenation activity and a low degree of acidity are best for maximizing hydroisomerization versus hydrocracking [122]. Figure 16 shows the conversion, cracking and recovery of diesel from feed. The pore opening of the molecular sieve can also have a major effect on the selectivity of this catalyst. If the pore opening is small enough to restrict the larger iso-paraffins from reacting at the acidic sites inside the

pore, the catalyst will show good selectivity for converting normal paraffin. The ideal catalyst for the selective hydroisomerization of n-paraffin should have both selectivity for isomerization, which comes from the proper balance of acidity and hydrogenation activity, and selectivity for reacting only with normal paraffins, which comes from the size of the pore opening of the molecular sieve used. However about carbenium ions and protolysis of protonic sites for isomerization are discussed in paper VI.

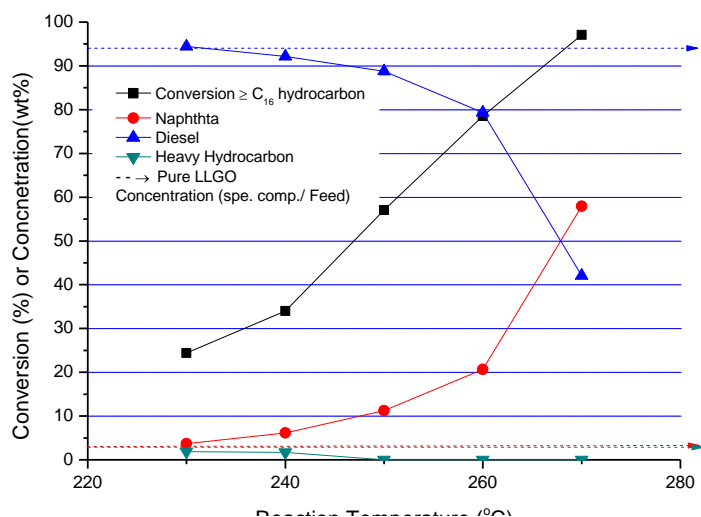


**Figure 16.** Hydroisomerization conversion and recovery at 250°C and 50 bar H<sub>2</sub> for 10wt% n-C<sub>16</sub> in Light gas oil.

### 6.3. Isomeric Lighter Fraction in Fuel Gas

As like longer hydrocarbon isomerization, the bimolecular pathway involves hydrogen transfer reactions that progressively lead to the disproportionation of alkenes to alkanes and aromatics. This reaction also contributes to the formation of coke. The gas fraction in fuel gas is presented in Paper VI. The yield shift implies conversion of linear and (mono) branched C<sub>6</sub>-C<sub>9</sub> alkenes (and, at first sight, also alkanes) to mostly propene and butenes, leaving the gasoline fraction enriched in aromatics and isopentenes. C<sub>5</sub>+ isomerization is not simply analogous to isomerization of C<sub>5</sub>+ alkenes because here a monomolecular isomerization step would call for a primary carbenium ion-like transition state with very high energy. Because this is seen as improbable, possible alternative mechanisms have been suggested, including a dimerization-isomerization-recracking mechanism and a mechanism involving intermediacy of adsorbed aromatic compounds via alkylation side chain isomerization-dealkylation. Further it makes more complicate in gas oil composition with dimerization-isomerization mechanism on similar as fuel gas estimation.



# CHAPTER 7

## Conclusion

### 7. Conclusion

The conclusions of articles are:

**Conclusion of Paper I and II:** During the hydrotreatment condition at moderate temperatures (300 to 370°C), the formation of higher hydrocarbon oxygenate groups, i.e. esters, acids and aldehydes had a 15 to 30% share (the rest contains gasoline, naphtha and unreacted feed). Further, cyclic group formation was observed, mainly as a product in gasoline fraction (distillate). Hydroprocessing at higher temperatures resulted in higher cracking and cyclic group formation. Moreover, isomeric and lighter cracking compounds mainly followed with radical groups formed from C-O detachment. Even viscosity adjustment through decomposition will play a crucial role in catalytic reaction conditions. To conclude, a longer pre-heated condition of any carboxylic group feed favors the catalytic operation as well as viscosity adjustment, but selectivity of C in the feed to product depends on the interfacial area and design of the pre-heating section. Higher concentrations of aldehyde formed from the carboxylic group results in the formation of CO in flue gas. Dodecanoic acid testing covers mainly CO<sub>2</sub> in the gas outlet. Our study clearly showed that CO<sub>2</sub> detachment from carboxylic acid radicals and CO from aldehyde radicals by C-C bond cleavage occurred. Further, the (C=O)-O bond cleavage was more favored than O-CH<sub>2</sub>.

**Conclusion of Paper III:** Mild pyrolysis, tested in a batch reactor in the presence or absence of H<sub>2</sub> and without a catalyst. This pre-heating test was to identify the carboxylic group variation. Here, both thermal treatment and catalytic treatment were studied. The presence of H<sub>2</sub> partial pressure in thermal treatment increases -C-O- bond breakage compared with N<sub>2</sub> atmosphere. H<sub>2</sub> limitation on the catalyst surface induces the catalytic and thermal reactions, but thermal cracking is less dominant after (C=O)-O detachment. Here, we conclude that the HDO is active on (C=O)-O- (carboxylic) scission and -(O=C)- (carbonyl) hydrogenation is

highly dominate in hydrotreatment (e.g., DCO and DCA). We found that the vegetable oil rate determines the temperature and bonding energy between C-C and C-O.

**Conclusion of Paper IV and V:** Aromatic content showed a steep increase in upgraded products at elevated temperatures. Furthermore, the data clearly indicate that the resin group had no influence on this increase. Paraffins to aromatic in LGO were found to significantly increase and the PAH concentration had a particularly strong influence on the quality of LGO. Upgrading resin acids and FAME increased the cetane number of LGOs, but domination of DCO and DCA needed to be controlled in elevated conditions. Upgraded LGO can be achieved to obtain <1 ppmw of sulphur with FAME and resin acids in LGO feed. Here, we found that deoxygenation and DCA had rate determining on resin acids hydroprocessing mechanism. The hydrogenation of the resin group showed some restriction by the hindrance of propyl and methyl groups on cyclic-ring. However, to some extent the PAH resin structure led to mono-aromatic by cyclic scission. Dehydrogenation, isomerization and polymerization are limited or not existing in this process. DCA only depends on temperature, whereas DCO depends on elevated temperature and space velocity.

The complete feed to product conversion was achieved for all space velocities and temperatures studied. The sulphur content of the upgraded product can achieve up to 1 to 3 ppmw. The observed variation of product selectivity was mainly by coke formation. The co processing route is possible with this low sulphur in the product to meet the needs of the downstream dearomatization. Aromatic content increases with temperature; in particular, PAH results in an upswing for higher temperature. The optimal condition depends on C<sub>18</sub> and C<sub>17</sub> formation and cloud point.

**Conclusion of Paper VI:**

Mono-branched isomers were present in all reaction conditions. However, the branched alkyl group has high impact in reducing the cloud point of diesel. As the reaction temperature is increased, the selectivity to di-branched isomers increases in the isomerized products with corresponding increase in naphtha. These results strongly suggest that di-branched isomers are mostly formed in successive reactions from mono-branched hydrocarbons. Selectivity of isomeric product at 250°C induces a favourable condition. Also, moderate reduction of aromatics in product illustrates the equilibrium condition with combination of bi-functional effect by catalyst in hydrogenation-dehydrogenation.

## **Overall Conclusion**

To conclude the thesis,

Thermally treated fat-rich material like rapeseed oil, FAME, tall oil has effect on temperature and contact time over inert material. Hence results achieved from 50 to 80% depend on contact time by consuming low hydrogen. This proves that pre-heated (350°C) fat-rich material relatively affected by interfacial surface contact on inert material to give thermally decomposed compounds with low consumption of hydrogen. Also, it proves to form isomeric and aromatic compound through radical reaction.

Followed with Catalytic hydro-processing of fat-rich material have yield hydroprocessed product on active catalyst by presence of sulphur and hydrogen. However, thermally decomposed product results into higher cracking with longer residence time. Thus, moderate temperature (350°C) with catalytic effect results to consume high hydrogen in hydroprocessing process for 100% conversion.

The hydro-isomerization process under  $\beta$ -H zeolite for hydroprocessed fat-rich material was tested. This process mainly depends on temperature and space velocity of feed. Increase in pressure and hydrogen intake proves to be beneficial, but limited to economical, process feasibility and catalyst life-time options. The overall results show better yield and 60 to 85% conversion at equilibrium temperature (250-260°C) with limited cracking for n-C<sub>16</sub> isomerization.

Overall observation results that non-catalytic thermal decomposition depends on temperature and space velocity of feed with limited influence on pressure and hydrogen parameters. On catalytic process, temperature and space velocity parameters influence the selectivity and yield of fat-rich feed, hence, pressure and hydrogen parameters partially enhance selectivity and yield by controlling product loss. Overall need of Hydrogen can be minimized from the favorable conditions.

## References

1. Dos Anjos, J. R. S.; Gonzales, W. A; Lam Y. L.; Frety, R.; Applied Catalysis, 1983, 5, 277-308.
2. [http://ec.europa.eu/energy/energy\\_policy/documents\\_en.htm](http://ec.europa.eu/energy/energy_policy/documents_en.htm). visited on 25th sep, 2007.
3. Gusmao, J.; Brodzki, D.; Djega-Mariadassou G.; Frety, R. Catalysis Today 1989, 5, 533-544.
4. EU strategy for bio-fuels, <http://europa.eu/scadplus/leg/en/lvb/l28175.htm>, Official Journal C 67 of 18 March 2006, visited on Sept, 04 2007.
5. Smejkal, Q.; Smejkalová, L; Kubicka, D. Chemical Engineering Journal 2009, 146 155–160.
6. Donnis, B.; Gottschalck R.; Peder Blom E.P.; and Knudsen, K.G. Top Catal 2009, 52, 229–240.
7. Lima, D.G.; Soares, V.C.D.; Ribeiro, E.B.; Carvalho, D.A.; Cardoso, É. C. V.; Rassi, F. C.; Mundim, K.C.; Rubim, J.C.; Suarez, P.A.Z. Journal of Analytical and Applied Pyrolysis 2004, 71, Issue 2, 987-996.
8. Senol, O.L.; Viljava, T.R.; Krause, A.O.I. Catalysis Today 2005, 106, 186-189.
9. Senol, O.L.; Ryymin, E.M.; Viljava, T.R.; Krause, A.O.I. Journal of Molecular Catalysis A: Chemical 2007, 268, Issue 1-2, 1-8.
10. Dupain, X.; Costa, D. J.; Schaverien C.J.; Makkee, M.; Moulijn, J.A. Applied Catalysis B: Environmental 2007 72, 44–61.
11. Filho, G.N.da R.; Brodzki, D.; Djega-Mariadassou, G. Fuel, 1993, 72, 4, 543-549.
12. Osmont, A.; Yahyaoui M.; Catoire, L.; Gökalp I.; Swihart, M. T. Combustion and Flame 2008, 155, 334-342.
13. Huber, G.W; O'Connor P.; Corma, A. Applied Cat A: General 2007, 329, 120-129.
14. Topsøe, H.; Clausen, B.C.; Massoth, F.E.; Hydro treating Catalysts: Science and Technology 1996, 22, 141–144.
15. Prochazkova, D; Zamostny, P; Bejblova, M; Cerveny, L; Cejka, J; Applied Catalyst (Gen), 2007, 332 (1) 56-64.
16. Corma, A.; Huber, G. W.; Sauvanaud, L.; O'Connor, P.; Journal of Catalysis 2007, 247, 307–327.
17. <http://www.dieselnet.com/standards/se/fuel.html>. visited on Sept, 04 2012.

18. Marker, T. J.P.; Kalnes, T.; McCall, M.; Mackowiak, D.; Jerosky, B.; Regan, B.; Nemeth, L.; Krawczyk, M.; Czernik, S.; Elliot, D.; Shonnard, D.; [http://www.osti.gov/energycitations/product.biblio.jsp?osti\\_id=861458](http://www.osti.gov/energycitations/product.biblio.jsp?osti_id=861458), 2005.  
**UOP, Des Plaines, Illinois.**
19. Maeki-Arevela, P.; Kubickova, I.; Snåre, M.; Eraenen, K.; Murzin, D.Yu. *Energy and Fuels* 2007, Vol. 21, 30-40.
20. Kubickova, I.; Snåre, M.; Eraenen, K.; Maeki-Arevela, P.; Murzin, D.Yu. *Catalyst Today* 2005, Vol.106, 197-200.
21. Chisholm, M.H.; Modeling the chemistry of hydrotreating; the hydrodesulphurization, hydrodenitrogenation, hydrodeoxygenation and hydrodemetallation of fossil fuels. *Polyhedron*, 1997, Vol.16 (18), 3071.
22. Rose, R.H.; Smith, D.R.; Vassallo, A.M.; *Energy and Fuels* 1993, Vol. 7, 319-325.
23. Ashida, R.; Painter, P.; Larsen, J.W; *Energy and Fuels* 2005, Vol. 19, 1954-1961.
24. Vassallo, A.M.; Attalla, M.I.J.; *Anal. Appl. Pyrol.* 1992, Vol. 23, 73-84.
25. Vlachos, N.; Skopelitis, Y.; Psaroudaki, M.; Konstantinidou, V.; Chatzilazarou, A.; Tegou, E.; *Analytica Chimica Acta*, 2006, Vol. 573-574, 459-465.
26. Balat, M; Balat, M; Kirtay, E.; Balat, H.; *Energy Conversion and Management* 2009, Vol.50, 3147-3157.
27. Palanisamy, S.; Anjun, W.M.; Gevert, B. Thermal reactions of rape seed oil with or without hydrogen, 7<sup>th</sup> Asia pacific Conference on Sustainable Energy and Environmental Technologies, October 15-19, 2009, Qingdao China.
28. Da Racha Filho, G.N.; Brodzki, D.; Djega-Mariadassou, G.; *Fuel*, 1993, Vol. 72(4), 543-549.
29. Stumborg, M; Wongb, A; Hogan, E; *Bioresource Technology* 1996, Vol. 56, 13.
30. Brunauer, S; Emmett, P.H.; Teller, E.; *J. Am. Chem. Soc.*,1938, Vol. 60, 309.
31. Solomon's, T.W.G.; *Organic Chemistry*, 5th ed., John Wiley & Sons, New York, 1992.
32. Alonso, J. S. J; Sastre, J.A. L; Romero-Avila, C.; Romero, E.J. L; *Fuel Processing Technology*, 2006, Vol. 87, 97-102.
33. Meher, L.C.; Vidya Sagar, D.; Naik, S.N.; Centre for Rural Development and Technology, Indian Institute of Technology Delhi, New Delhi 110016, India.
34. Santacesaria, E.; Parrella, P.; Di Sergio M.; Borrelli, G.; *Appl. Catal. A*, 1994, Vol. 116, 269.

35. Fernández, M. B.; Tonetto, G M.; Crapiste, G. H.; Ferreira M. L.; Damiani, D. E.; *Journal of Molecular Catalysis A: Chemical*, 2005, Vol. 237, 67–79.
36. Fernández, M. B.; Piqueras, C. M.; Tonetto, G M.; Crapiste, G. H.; Ferreira M. L.; Damiani, D. E.; *Journal of Molecular Catalysis A: Chemical*, 2005, Vol. 233, 133–139.
37. Huber, G. W.; O'Connor, P.; Corma, A; *Applied Cat (A) general*; 2007.
38. Lisitsyn, A.S.; *App. Cat (A) General* 2007.
39. Chen, Y.Z.; Wu, K.J.; *Applied catalyst*, 1991, Vol.78.
40. Zhao, Y.; *Mechanisms of Hydro denitrogenation of Amines over Sulphide NiMo, CoMo, and Mo Supported on Al<sub>2</sub>O<sub>3</sub>*, *PhD thesis*, Zürich, 2004.
41. Byskov, L. S.; Norskov, J. K.; Clausen B. S.; Topsøe, H.; *Journal Of Catalysis*, 1999, Vol 187.
42. Mitchel, R.H.; Lai, Y.; *Tetrahedron Letter*, 1980, 2637.
43. Prochazkova, D.; Zamostny, P.; Bejblova, M.; Cervený, L.; Cejka, J.; *Applied Catalyst (Gen)*, 2007, Vol. 332.
44. Dupain, X.; Costa, D. J.; Schaverien, C. J.; Makkee, M.; Moulijn, J. A.; *Applied Catalysis B: Environmental*, 2007, Vol. 72, 44–61.
45. Long, F.X.; Gevert, B. S.; *Journal of Catalysis*, 2004, Vol. 222(1), 1-5.
46. Ono, Y.; *Catalysis Today*, 2003, Vol. 81, 3–16.
47. Taylor, R. J.; Petty, R. H.; *Applied Catalysis A: General*, 1994, Vol. 119, 121-138.
48. Weitkamp, J.; Gould, R.F.; *Am. Chem. Soc. Symposium Series No. 20*, Washington DC, 1975, 1.
49. Jae, J.; Tompsett, G. A.; Foster, A. J.; Hammond, K. D.; Auerbach, S. M.; Lobo, R.F.; Huber, G. W.; *Journal of Catalysis*, 2011, Vol. 279(2), 257–268.
50. Zabaniotou, A.; Ioannidou, O.; Skoulou, V.; *Fuel*, 2008, Vol. 87 (8-9), 1492-1502.
51. Demirbas, A.; *Energy and Combustion Science*, 2007, Vol. 33, 1-18.
52. Thuijl, E.V.; Ross. C.J.; Beurskens, L.W.M.; An overview of biofuel technologies, markets and policies in Europe. [www.ecn.nl/docs/library/report/2003/c03008.pdf](http://www.ecn.nl/docs/library/report/2003/c03008.pdf), 2003.
53. Naik, S.N.; Goud, V. V.; Rout, P. K.; Dalai, A. K.; *Renewable and Sustainable Energy Reviews*, 2010, Vol. 14, 578-597.
54. Pawelec, B.; Navarro, R. M.; Campos-Martin, J. M.; Fierro, J. L. G.; *Catalysis Science & Technology*, 2011, Vol. 1, 23-43.

55. Vyas, A.P.; Verma, J. L.; Subrahmanyam, N.; Fuel, 2009, Vol. 89(1), 1-9.
56. Šimáček, P.; Kubicka, D.; Šebor, G.; Pospíšil, M.; Fuel, 2010, Vol. 89, 611-615.
57. Murti, S.D.S.; Choi, K.; Sakanishi, K.; Okuma, O.; Korai, Y.; Mochida, I.; Fuel, 2005, Vol. 84(2-3), 135-142.
58. Donniss, B., Egeberg, R. G.; Blom, P.; Knudsen K. G., Top Catal., 2009, Vol. 52, 229-240.
59. Yakovlev, V.A., Khromova, S.A.; Sherstyuk, O.V.; Dundich, V.O.; Ermakov, D.Y.; Novopashina, V.M.; Lebedev, M.Y.; Bulavchenko, O.; Parmon, V.N. , Catalysis Today, 2009. Vol. 144, 362-366.
60. Huang, W.; Li, D.; Kang, X.; Shi, Y; Nie, H; Research Institute of Petroleum Processing, SINOPEC, Beijing 100083, China, Studies in Surface Science and Catalysis, Vol. 154.
61. Deng, P; Nie, C; Li; Q. Z.; Journal of Fudan University (Natural Science) 2001, Vol.40 (4), 387–391.
62. Blasco, T.; Chica, A.; Corma, A.; Murphy, W. J.; Agundez-Rodríguez, J; Pérez-Pariente. J.; Journal of Catalysis, 2006, Vol. 242 (1), 153–161.
63. Ren, X.T.; Li, N.; Cao, J.Q.; Wang, Z. Y.; Liu, S.Y.; Xiang, S. H.; Applied Catalysis A: General, 2006, Vol. 298, 144–151
64. Serrano-Ruiz, J.C.; Dumesic, J. A.; Energy Environmental Science, 2011, Vol. 4, 83-99.
65. Speight, J.G., Handbook of Petroleum Product Analysis. John Wiley & Sons, 2002.
66. Tiwari, R.; Rana, B. S.; Kumar, R.; Verma, D.; Kumar, R.; Joshi, R. K.; Garg, M. O.; Sinha, A. K.; Catalysis Communications, 2011, Vol. 12(6), 559-562.
67. Monnier, J.; Tourigny, G.; Soveran, D. W.; Wong, A.; Hogan, E.N.; Stumborg, M.; USA 5705722, Natural Resources Canada, 1998.
68. Delmon, B.; Froment, G.F.; Grange, P.; Hydrotreatment and hydrocracking of oil fractions: proceedings of the 2nd international symposium/7th European workshop, Antwerpen, Belgium, November 14-17, 1st ed. Studies in surface science and catalysis, ed. G.F.F. B. Delmon, P. Grange. 1999, Amsterdam [Netherlands] ; New York: Elsevier. xi, 446.
69. Kubicka, D.; Kaluza, L.; Applied Catalysis A: General, 2010, Vol. 372, 199-208.
70. Le Bihan, L.; Yoshimura, Y.; Fuel, 2002, Vol. 81(4), 491-494.

71. Melero, J.A.; Clavero, M. M.; Calleja, G.; García, A.; Miravalles, R.; Galindo, T., *Energy & Fuels*, 2009, Vol. 24(1), 707-717.
72. Senol, O.I.; Ryymin, E. M.; Viljava, T. R.; Krause, A. O. I.; *Journal of Molecular Catalysis A: Chemical*, 2007, Vol. 268, 1-8.
73. Viljava, T.R.; Komulainen, R.S.; Krause, A.O.I.; *Catalysis Today*, 2000, Vol. 60, 83-92.
74. Bruice, P.Y.; *Organic Chemistry*, 6<sup>th</sup> Edition, Pearson Hall, 2011.
75. Senol, O.I.; Viljava, T. R.; Krause, A. O. I.; *Applied Catalysis A: General* 2007, Vol. 326, 236-244.
76. Senol, O.I.; Viljava, T. R.; Krause, A. O. I.; *Catalysis Today*, 2005, Vol. 106, 186-189.
77. Senol, O.I.; Viljava, T. R.; Krause, A. O. I.; *Catalysis Today*, 2005, Vol. 100, 331-335.
78. Senol, O.I.; Ryymin, E. M.; Viljava, T. R.; Krause, A. O. I.; *Journal of Molecular Catalysis A: Chemical*, 2007, Vol. 277, 107-112.
79. Wadlinger, R. L. ;Kerr, G. T.;Rosinski, E. J. Catalytic composition of a crystalline zeolite, United States Patent, 3308069, 1967.
80. Badilla-Ohlbaum, R.; Chadwick, D.; Gavin, D. G.; *Fuel*, 1981, Vol. 60(5), 452-453.
81. Maher, K.D., Kirkwood, K. M.; Gray, M. R.; Bressler, D. C., *Ind. Eng. Chem. Res*, 2008, Vol. 47, 5328-5336.
82. Ashida, R.; Painter, P.; Larsen, J. W.; *Energy & Fuels*, 2005, Vol. 19, 1954-1961.
83. Osmont, A.; Yahyaoui, M.; Catoire, L.; Gokalp, I.; Swihart, M. T.; *Combustion and Flame*, 2008, Vol. 155(1-2), 334-342.
84. Osmont, A.; Catoire, L.; Gokalp, I.; Swihart, M. T.; *Energy & Fuels*, 2007, Vol. 21(4), 2027-2032.
85. Curey, F.A.; Sundberg, R. J.; Kluwer, M.; Academic/Plenum Publishers, 2000. Fourth Edition.
86. Turpeinen, E.; Sapei, E.; Uusi-Kyyny, P.; Keskinen, K. I.; Krause, O. A. I.; *Fuel*, 2011, Vol. 90(11), 3315-3322.
87. Kubicka, D.; Horacek, J.; *Applied Catalysis A: General*, 2011, Vol. 394(1-2), 9-17.
88. Rollmann, L.D.; *Journal of Catalysis*, 1977 Vol. 46, 243-252.

89. Prielcel, P.; Kubicka, D.; Capek, L.; Bastl, Z.; Rysanek, P.; *Applied Catalysis A: General*, 2011, Vol. 397(1-2), 127-137.
90. Prielcel, P.; Kubicka, D.; Capek, L.; Bastl, Z.; Homola, F.; Rysanek, P.; Pouzar, M., *Catalysis Today*, 2011, Vol. 176(1), 409-412.
91. Graca, I.; Fernandes, A.; Lopes, J. M.; Ribeiro, M. F.; Laforge, S.; Magnoux, P.; Ramoa Ribeiro, F.; *Fuel*, 2011, Vol. 90(2), 467-476.
92. El-Nahas, A.M.; Navarro, M. V.; Simmie, J. M.; Bozzelli, J. W.; Curran, H. J.; Dooley, S.; Metcalfe, W.; *The Journal of Physical Chemistry A*, 2007, Vol. 111(19), 3727-3739.
93. Galuszka, J.; Chang, J. R.; Amenomiya, Y.; Seivama, T.; Tanabe, K.; *Studies in Surface Science and Catalysis*. 1981, Elsevier, 529-541.
94. Mohan, D; C.P.; Steele, P; *Energy & Fuels*, 2006, Vol. 20, 848-889.
95. Czernik, S.; Bridgwater, A. V.; *Energy & Fuels*, 2004, Vol. 18(2), 590-598.
96. Lapuerta, M.; Armas, O.; Rodríguez-Fernández, J.; *Progress in Energy and Combustion Science*, 2008, Vol. 34(2), 198-223.
97. Teh, C. H.; *Catalysis Today*, 2004, Vol. 98(1-2), 3-18.
98. Demirbas, A.; *Energy and Combustion Science*, 2007, Vol. 33, 1-18.
99. Demirbas, A.; *Fuel*, 2008, Vol. 87, 1743-1748.
100. Monnier, J.T.; G.; Soveran, D. W.; Wong, A.; Hogan, E. N.; Stumborg, M.; USA 5705722, Natural Resources Canada, 1998.
101. Robert Coll, S.U.; Jacoby, W. A.; *Energy & Fuels*, 2001, Vol. 15, 1166-1172.
102. Laza, T.; Bereczky, A.; *Fuel*, 2011, Vol. 90(2), 803-810.
103. Ghosh, P.; *Energy & Fuels*, 2008, Vol. 22(2), 1073-1079.
104. Hashimoto, K.; Ikeda, M.; Arai, M.; Tamura, M.; *Energy & Fuels*, 1996, Vol. 10(6), 1147-1149.
105. Yakovlev, V.A.; S.A.K.; Sherstyuk, O.V.; Dundich, V.O.; Ermakov, D.Yu.; Novopashina, V.M.; Lebedev, M.Y.; Bulavchenko, O.; Parmon, V.N.; *Catalysis Today*, 2009, Vol. 144, 362-366.
106. Alonso, J.S.J.; Sastre, J. A. L.; Romero-Avila, C.; Lopez, E.; *Biomass and Bioenergy*, 2008, Vol. 32(9), 880-886.
107. Maki-Arvela, P.; Snåre, M.; Eranen, K.; Murzin, D. Y.; *Energy & Fuels*, 2007, Vol. 21, 30-41.
108. Breda, K.; *Fuel*, 2008 Vol. 87(7), 1306-1317.

109. Chen, X.L.; Yongbin; Shao; Qun; Shiyou Yu Tianranqi Huagong, 2010, Vol. 39(6), 491-493.
110. Topsøe, H.; Hinnemann, B.; Norskov, J. K.; Lauritsen, J. V.; Besenbacher, F.; Hansen, P. L.; Hytoft, G.; Egeberg, R. G.; Knudsen, K. G.; *Catalysis Today*, 2005, Vol. 107-108(0), 12-22.
111. Bauer, F.; Johansson, P.; Lindén, J.; Nyström, M.; Rudén, L.; Tallolja som biobaserad dieselsättning- Katalytisk hydrogenering av hartssyror. Kandidatarbete inom Kemiteknik, Chalmers Tekniska Högskola, Göteborg, 2010. KBTX01-10-6.
112. Snare, M.; Maki-Arvela, P.; Chichova, D.; Eranen, K.; Murzin, D.Yu.; *Fuel*, 2008, Vol. 87, 933-945.
113. Snare, M.; Maki-Arvela, P.; Eranen, K.; Warna, J.; Murzin, D.Yu.; *Chemical Engineering Journal*, 2007, 134, 29-34.
114. Badilla-Ohlbaum, R.; Chadwick, D.; Gavin, D. G.; *Fuel*, 1981, Vol. 60(5), 452-453.
115. Graham, R.G.; *Biomass and Bioenergy*, 1994, Vol. 7(1-6), 251-258.
116. Donnis, B.; Egeberg, R. G.; Blom, P.; Knudsen K. G.; *Top Catal.*, 2009, Vol. 52, 229-240.
117. Kubickova, I.; Eranen, K.; Maki-Arvela, P.; Murzin, D. Y.; *Catalysis Today* 2005, Vol. 106, 197-200.
118. Idem, R. O.; R.K, S.P.; Bakhshi, N. N.; *Fuel Processing Technology*, 1997, Vol. 51, 101-125.
119. Osmont, A.; Catoire, L.; Dagaut, P.; *The Journal of Physical Chemistry A*, 2009, Vol. 114(11), 3788-3795.
120. Senol, O.I.; R, E.M.; Viljava, T.R.; Krause, A.O.I.; *Journal of Molecular Catalysis A: Chemical*, 2007, Vol. 277, 107-112.
121. Hanks, P.L.; Lewis, W.E.; Cole, K.Y.; A.C. Society, 2010: USA, 30.
122. Anpo, M; Onaka, M; Yamashita, H; *Surface and Technology Catalysis*, 2002, Vol. 145, 63-70.
123. Simon-Masseron, A.; Marques, J.P.; Lopes, J.M.; Ribeiro, F.R; Gener, I.; Guisnet, M.; *Applied Catalysis A: General*, 2007, 316, 75–82.

## 8. Acknowledgments

This work was conducted at the Surface Chemistry Department, Chalmers University of Technology and financially supported by *Preem AB* and *Swedish Energy Agency*.

Special thanks to *Preem AB*, Sweden for the feedstock support.

I would like to express my deepest gratitude to all persons who have contributed in some way to this thesis. I would especially like to thank the following individuals:

First, I would like to thank my supervisor, *Associate Professor Börje S. Gevert*, for welcoming me to the department and for all his support and sound advice over the years.

*Professor Krister Holmberg*, my examiner, for giving me the opportunity to complete my doctoral thesis.

*Associate professor Hanna Härelind*, my co-supervisor, for excellent guidance and for all her help with the Drift-FTIR work.

*Eva Lind Grennfelt*, Preem AB, for sharing conceptual study.

Special thanks to the Preem Petroleum laboratory staff for performing some of the analytical work.

*Dr. Mayi*, my former colleague, for help with the SEM analysis.

*Dr. Zebastian Bohström*, my former colleague, for discussions and support in TEM analysis.

*Ann Jakobsson*, for her help with all the administrative work.

*Lars-Ove Olsson*, Nestejacobs AB, for sharing his experience and knowledge about refinery, and an inspiring personality.

*Johan Bengtsson VD*, Nestejacobs AB, for encouragement.

Thanks to all the Nestejacobs Colleagues for creating a wonderful atmosphere in short duration.

I would also like to thank my former students at Chalmers: *Arshad, Manu, Estela, Oliver, Manual, Yuan, Kiran, Ali, Talut, Alan, Alborz, Caroline, Karin, Younis* and *Amir* for their valuable thesis work.

I am grateful to *Dr. Ahmad Kalantar*, Nynäs Naphthenic AB, for his support and valuable ideas that were needed in order to start good research work.

My friends, *Sandeep Shetty*, Volvo cars, and *Kranthi Kumar*, Saybolt AB, who are best friends to share my time on leisure period.

*Nina Kirilova* and *Anna Kirilova*, special thanks for their affection and moral support.

Finally, all my gratitude goes to my family for their affection, patience, encouraging attitude and support. Special thanks to my brother-in law, *S. Mohan*, for his support.

*Lana Kirilova MSc.*, be a part of my life with affection and huge support in enthusiasm.

I would like to dedicate this thesis to my grandfather *Late Kolandaipayan*, who was the first person support me for higher education.

Göteborg, March 2013.

**Shanmugam Palanisamy**

